HELSINKI UNIVERSITY BIOMEDICAL DISSERTATIONS NO. 71

BIOPHYSICAL STUDIES ON CATIONIC LIPOSOMES

– IMPLICATIONS FOR SELF-ASSEMBLY AND MECHANISM OF LIPOFECTION

Samppa Ryhänen

Helsinki Biophysics & Biomembrane Group
Institute of Biomedicine/Biochemistry
Faculty of Medicine
University of Helsinki
Finland

Academic Dissertation

To be presented with the assent of the Faculty of Medicine of the University of Helsinki for public examination in the Small Lecture Hall of Haartman Institute, Haartmaninkatu 3, Helsinki on 5th January 2006, at noon.

Helsinki 2006

SUPERVISED BY

Professor PAAVO KINNUNEN
Biophysics and Biomembrane Group
Institute of Biomedicine/Biochemistry
University of Helsinki
Helsinki, Finland

REVIEWED BY

Professor OLLI IKKALA
Department of Engineering Physics and Mathematics
Helsinki University of Technology
Espoo, Finland

Docent MARTIN HOF
J. Heyrovský Institute of Physical Chemistry
Academy of Sciences of the Czech Republic
Prague, Czech Republic

OPPONENT

Docent JARMO WAHLFORS
Department of Biotechnology and Molecular Medicine
University of Kuopio
Kuopio, Finland

ISBN 952-10-2847-5 (paperback)
ISBN 952-10-2848-3 (PDF)
ISSN 1457-8433
http://ethesis.helsinki.fi/

Helsinki 2005
Yliopistopaino

To Eeva

CONTENTS

ABBREVIATIONS

A	area per molecule
$A_{lift\text{-}off}$	lift-off area
ATR	attenuated total reflectance
c_A, [A]	concentration of compound A
CL	cationic lipid
CMC	critical micellar concentration
CT-DNA	calf thymus DNA
DAG	diacylglycerol
DHAB	dihexadecyldimethylammonium bromide
DMEM-10	Dulbecco's modified Eagle's medium with 10% fetal calf serum
DMEM-SF	serum free Dulbecco's modified Eagle's medium
DMPC	1,2-dimyristoyl-*sn*-glycero-3-phosphocholine
DMTAP	dimyristoyltrimethylammonium propane
DOPE	1,2-dioleoyl-*sn*-glycero-3-phosphoethanolamine
DPH-PC	2-(3-(diphenylhexatrienyl)propanoyl)-1-hexadecanoyl-*sn*-glycero-3-phosphocholine
DSC	differential scanning calorimetry
EDTA	ethylenediaminetetraacetic acid
EGFP	enhanced green fluorescent protein
EtBr	ethidium bromide
FTIR	Fourier transform infrared
GV	giant vesicle
ΔH	enthalpy of phase transition
Hepes	N-(2-hydroxyethyl)piperazine-N'-2-ethanesulfonic acid
L_α	lamellar disordered fluid phase
L_β	lamellar ordered gel phase
LUV	large unilamellar vesicle

M-1	(2R,3S)-2,3-dimethoxy-1,4-bis(N-hexadecyl-N,N-dimethylammonium)butane dibromide
MLV	multilamellar vesicle
NMR	nuclear magnetic resonance
P_β	ripple gel phase
PC	phosphatidylcholine
PE	phosphatidylethanolamine
PEI	polyethyleneimine
PEG	polyethylene glycol
POPC	1-palmitoyl-2-oleoyl-*sn*-glycero-3-phosphocholine
r	fluorescence emission anisotropy
SCID	severe combined immunodeficiency
T	temperature
T_g	transition temperature after which large giant vesicles appear
T_m	main transition temperature
T_p	pretransition temperature
T_s	transition temperature after which small giant vesicles appear
X_A	mole fraction of compound A
γ	surface tension
λ_c	wavelength at spectral center of mass
π	surface pressure
$\upsilon_s CH_2$	$-CH_2-$ symmetric stretching mode
$\upsilon_{as} CH_2$	$-CH_2-$ antisymmetric stretching mode

ABSTRACT

Cationic liposomes interact spontaneously with anionic DNA by virtue of electrostatic attraction forming complexes ("lipoplexes") that carry nucleic acid into eukaryotic cells in which gene coded by DNA is expressed. Efficient, reliable, and above all safe gene transfer vectors are required in order to utilize the vast amount of genetic information in gene therapeutics. Safety concerns have raised doubt about the future of viral gene transfer and thus the need for synthetic gene transfer tools with improved safety has been emphasized. Liposomal transfection is one of the most promising rivals for viral gene transfer. Yet, similarly to all present non-viral transfection systems liposomes convey genes into cells significantly less efficiently than viruses. To alleviate this problem qualities of lipoplexes have been extensively studied to establish rational basis for lipoplex design.

This study was focused to elucidate the properties of cationic liposomes in settings relevant to liposomal transfection and self-assembly of cationic amphiphiles in general. More specifically, the impact of surface charge density on transfection efficiency in cell cultures, the mode of interaction with DNA, and molecular organization within the lipid bilayer was investigated for binary liposomes consisting of cationic lipid dihexadecyldimethylammonium bromide (DHAB) and zwitterionic dimyristoylphosphatidylcholine (DMPC). Moreover, the effect of NaCl on the self-assembly of DHAB/DMPC liposomes as well as vesicles made of cationic gemini surfactant was assessed.

The transfection efficiency of DHAB/DMPC liposomes complexed with plasmid DNA was critically dependent on the molar fraction of DHAB (X_{DHAB}) in the liposomes. Accordingly, vesicles with $X_{DHAB} \geq 0.50$ demonstrated efficient transfection while only negligible transgene expression was measured for vesicles with lower mole fraction of DHAB. Varying surface charge density had significant impact also on the properties of DHAB/DMPC membranes and their interaction with DNA. Only liposomes with $X_{DHAB} > 0.50$ induced DNA condensation as observed by static light scattering and ethidium bromide intercalation assay. Furthermore, the main transition temperature (T_m) of DHAB/DMPC vesicles followed a sigmoidal dependence on X_{DHAB} suggesting significant changes in the organization of membrane lipids due to varying surface charge density. Initial increase in T_m until a maximum at $X_{DHAB} = 0.40$ is explained by pairing of cationic headgroup of DHAB and zwitterionic phosphocholine headgroup and subsequent electrostatic reorientation of P^-N^+ dipole from horizontal to more vertical conformation in respect to bilayer plane. This reorientation results in diminished mean molecular areas occupied by the lipids that cause increment in T_m due to augmented chain-chain interactions in the hydrocarbon phase of the bilayer. As the mole fraction of DHAB is further elevated the number of unpaired DHAB molecules increases and Coulombic repulsion expands the membrane evident as decrement in T_m. However, at $X_{DHAB} > 0.60$ the decrease in T_m halted despite even increasing surface charge. Fourier transform infrared and fluorescence spectroscopy suggested surface charge density induced phase transition from classical lipid bilayer into interdigitated phase that

provides explanation for observed behavior as interdigitation allows for cationic headgroups to maximize their distance and simultaneously results in tight packing of acyl chains in the hydrocarbon phase of the bilayer. Addition of NaCl into buffer reverted normal bilayer packing thus confirming electrostatic repulsion as a driving force for the observed interdigitation.

Cationic gemini surfactant M-1 demonstrated a sequence of mesoscale transitions at specific temperatures in the presence of high NaCl concentration. More specifically, upon heating first a transition from submicroscopic structures to large tubules and giant vesicles is evident after which another transition to numerous population of smaller, homogenous giant vesicles was seen. It is suggested that cationic headgroup of gemini surfactant with fixed distance between charges acts as a nucleation center for a commensurate counterion lattice that forms onto surface of the membrane. Planarity of this Cl^- ion lattice favors formation of giant vesicles instead of smaller lipid aggregates with higher membrane curvature.

To summarize, surface charge density was shown to be an important determinant for efficiency of liposomal transfection. The underlying mechanism for the above observation is the ability of liposomes with high surface charge density to condense plasmid DNA and disrupt the endosomal membrane wherein latent tendency of these vesicles to form interdigitated phase could be of importance. Furthermore, spontaneous formation of giant vesicles by cationic gemini surfactant that was dependent on both NaCl concentration and temperature was described. To explain this remarkable mesoscale transition a novel mechanism controlling curvature of charged lipid membranes by a commensurate counterion lattice is proposed.

ORIGINAL PUBLICATIONS

This thesis is based on following original publications, referred to in the text by Roman numerals I-IV.

I. Samppa J. Ryhänen, Matti J. Säily, Tommi Paukku, Stefano Borocci, Giovanna Mancini, Juha M. Holopainen, and Paavo K. J. Kinnunen. Surface charge density determines the efficiency of cationic gemini surfactant based lipofection. *Biophysical Journal* **84** (2003) 578-587.*

II. Samppa J. Ryhänen, Juha-Matti I. Alakoskela, and Paavo K. J. Kinnunen. Increasing surface charge density induces interdigitation in vesicles of cationic amphiphile and phosphatidylcholine. *Langmuir* **21** (2005) 5707-5715.

III. V. Matti J. Säily, Samppa J. Ryhänen, Juha M. Holopainen, Stefano Borocci, Giovanna Mancini, and Paavo K. J. Kinnunen. Characterization of mixed monolayers of phosphocholine and a dicationic surfactant SS-1 with a Langmuir balance: Effects of DNA. *Biophysical Journal* **81** (2001) 2135-2143.*

IV. Samppa J. Ryhänen, V. Matti J. Säily, Mikko J. Parry, Paola Luciani, Giovanna Mancini, Juha-Matti I. Alakoskela, and Paavo K. J. Kinnunen. A novel mesoscale lipid phase transition from small submicroscopic vesicles to cytomimetic membrane assemblies. *Manuscript.*

Publication III will be used also as a part of the dissertation of MD Matti Säily.

* Correction article regarding structure of the cationic lipid used in these articles was published in *Biophysical Journal* **89** (2005) 753 (see Original Publications section for details). Nomenclature described in correction article is used in this thesis.

1. INTRODUCTION

"In biology, if seeking to understand function, it is usually a good idea to study structure."

–Francis Crick

Liposomal transfection (“lipofection”) utilizing complexes of cationic liposomes and plasmid DNA ("lipoplexes") represents safe, reliable, and easy-to-use means to introduce foreign genetic material into eukaryotic cells. Since its introduction (Felgner et al., 1987) lipofection has become the most popular transfection method *in vitro*. Major drawback of lipofection is limited transfection efficiency hampering its usage particularly in settings more complex than cell cultures, such as gene delivery *in vivo*. Current lipoplex design is to large extent based on trial and error. Thus much better efficacy could be expected if lipoplexes were constructed rationally employing detailed knowledge on structure-function relationship. Yet, exploring critical parameters determining efficiency of lipofection is not an easy task. While lipoplexes themselves are exceedingly complex self-assembling systems consisting of positively charged lipid membranes and highly charged anionic polyelectrolyte, their flurry interplay with eukaryotic cells, involving e.g. interactions with cellular lipid membranes and intracellular trafficking, makes rational approach to lipofection truly challenging. Attempt to elucidate mechanism of the lipofection is based on long tradition of interdisciplinary biomembrane research providing basic information on the structure and dynamics of lipid membranes as well as efficient experimental tools to characterize interactions of cationic liposomes and DNA. Intensive research efforts during last decade have revealed many important parameters of lipoplexes affecting their properties as transfection vectors but the big picture is still incomplete (Zuhorn and Hoekstra, 2002; Elouahabi and Ruysschaert, 2005).

Studies on cationic liposomes mainly motivated by practical and economical interest due to their use in lipofection have revealed also interesting novel features of biological membranes as well as laid road for other applications of liposomes. Lipids bearing net electric charge are ubiquitous building blocks of biomembranes and their distribution is strictly

controlled by the cell implying for functional importance. More specifically, anionic lipids are known to be involved in a range of cellular processes such as signal transduction, membrane-protein interactions, and structural transitions of biomembranes (Langner and Kubica, 1999), and natural cationic lipid sphingosine is present in nuclear membranes and readily interacts with DNA altering its conformation and forming ternary complexes with DNA and histones (Kõiv and Kinnunen, 1994; Kõiv et al., 1995).

In the present study mixed lipid membranes consisting of cationic lipid dihexadecyldimethylammoniumbromide (DHAB) and phospholipids, their interactions with DNA, and transfection properties as complexes with plasmid DNA were characterized with special emphasis on impact of surface charge density. In addition, self-assembly of a cationic gemini surfactant in the presence of NaCl was studied and a rapid temperature induced transition from submicroscopic structures into giant vesicles was described. The thesis will open with review of literature briefly describing biological and physical properties of lipid membranes and current knowledge on mechanism of lipofection. In the next section experimental techniques used are outlined followed by results obtained from the experiments. Discussion encloses the thesis by placing results in the context of previous literature and introducing conclusions of the study.

2. REVIEW OF THE LITERATURE

2.1 LIPOSOMES, LIPID MONOLAYERS, AND CELLULAR MEMBRANES

Lipid bilayer is the basic structure whereon proteins and carbohydrates assemble to form functional cellular membranes. Plasma membrane is probably the best known example of cellular membrane as it provides the semipermeable barrier that separates a cell from its surroundings. Moreover, eukaryotic cells are virtually packed with various membrane structures because lipid bilayers constitute also the structural framework of cellular organelles, such as mitochondria, nucleus, Golgi apparatus, and endoplasmic reticulum, crowding the intracellular space (Alberts et al., 2002). Classically lipid membranes have been described by so-called fluid-mosaic model as two-dimensional fluid providing structural matrix for peripheral and integral membrane proteins (Singer and Nicolson, 1972). However, in addition to structural function a more dynamic view on lipid membranes has emerged as their active role in the cell physiology is being revealed (Mouritsen, 2005). A key feature of lipid membranes is their self-assembly in aqueous solution from chemically diverse collection of lipids producing dynamic structure that shows pleomorphic phase behavior (Kinnunen and Laggner, 1991) and biologically relevant functional ordering (Kinnunen, 1991; Mouritsen and Kinnunen, 1996; Simons and Ikonen, 1997). Because biomembranes with incorporated protein and carbohydrate structures are extremely complex molecular assemblies studying them calls for interdisciplinary approach requiring expertise e.g. in cell biology, soft matter physics, biochemistry, and organic chemistry (Mouritsen, 2005). Lipid membranes are important also as innovative materials in various technical applications, such as controlled release drug delivery (Allen and Cullis, 2004) and nanotechnology (Evans et al., 1996), requiring sophisticated self-assembly of constituents.

2.1.1 Self-assembly of lipids

Spontaneous assembly of lipids is mainly driven by the hydrophobic effect organizing amphiphilic lipid molecules so as to minimize entropically unfavorable interactions between hydrophobic acyl chains with surrounding water and is further fine-tuned by various intermolecular forces such as electrostatic interactions, hydrogen bonding, as well as van der Waals and dispersion forces (Israelachvili, 1991). Lipid packing into small scale 3-D structures is governed by effective shape of the lipid that is determined by van der Waals volume and geometry of the molecule as well as hydration shell, conformation, and intermolecular forces acting on a molecule (Kinnunen, 1996). This relationship is generally described by packing parameter p defined as (Israelachvili et al., 1980)

$$p = \frac{v}{al}$$

where v is the volume of hydrocarbon chain(s), a area occupied by the headgroup, and l the maximum length of hydrocarbon chains. Accordingly, conventional spherical micelles are formed when molecule preferentially adopts conical shape, i.e. $p < 1/3$, and non-spherical (e.g. rod-like or discoidal) micelles form when molecular geometry resembles truncated cone with $1/3 < p < 1/2$ (Fig. 2.1). Alternatively, very large headgroup area compared to area occupied by acyl chains can drive bilayer into chain interdigitated phase as the energetic penalty of exposing acyl chains to aqueous phase is counterbalanced by increased separation of bulky headgroups (Pascher et al., 1992). Biologically most important mode of lipid

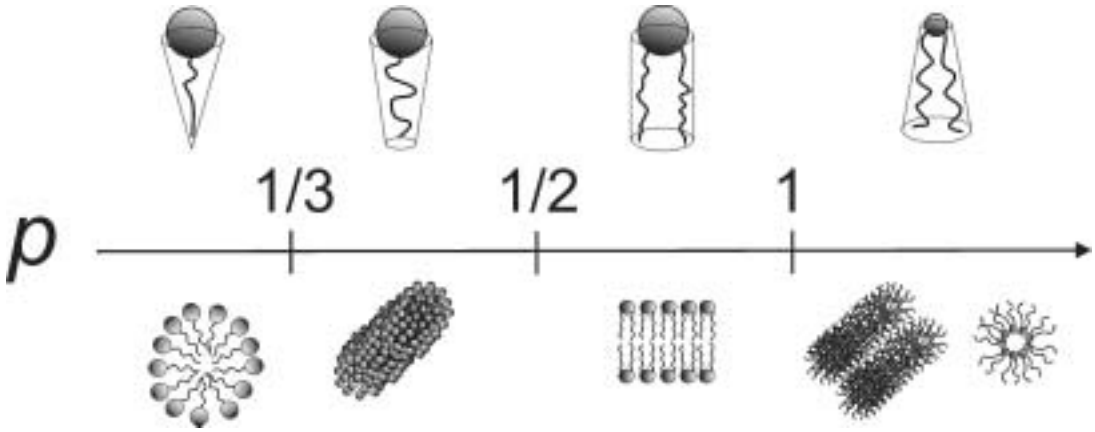

FIGURE 2.1 Schematic illustration of the impact of packing parameter p on lipid assemblies formed in aqueous solution. See text for details.

packing, lipid bilayer, requires nearly cylindrical molecular shape with $1/2 < p < 1$. If $p > 1$ inverted structures with negative spontaneous curvature (e.g. inverted micelles or inverted hexagonal phase) form.

2.1.2 Model membranes

Because of the enormous complexity of natural biomembranes simplified model membranes are used to characterize properties of lipids and their supramolecular aggregates. Liposomes (Fig. 2.2, panel A) have been the most popular model system in lipid research since Bangham and co-workers described that phospholipids form closed multilamellar vesicles in aqueous solution (Bangham et al., 1965). Dispersing phospholipids in water yields a population of multilamellar liposomes (MLVs) that is heterogeneous both in size and shape. This is undesirable for many applications and generally more homogenous liposome population is achieved by exposing lipid dispersion to either ultrasonication so as to obtain small unilamellar vesicles (SUVs, diameters approx. 30 nm) or extrusion through polycarbonate filters with small pores to yield large unilamellar vesicles (LUVs, diameters approx. 50-200 nm, depending on pore diameter). Eukaryotic cells have typically diameters of approx. 10-20 μm being much larger than SUVs or LUVs. Size difference may cause bias in experiments, which are sensitive to membrane curvature and lipid packing conditions. To this end, giant unilamellar vesicles (GUVs), prepared e.g. by electroformation (Angelova and Dimitrov, 1986) or solid hydration method (Menger and Gabrielson, 1995), with diameters from 5 to 200 μm represent more cytomimetic model system (Menger and Keiper, 1998; Menger and Angelova, 1998; Holopainen et al., 2003).

Amphiphilic lipids form spontaneously a monomolecular film when carefully deposited on the air/water interface in evaporating organic solvent (Fig. 2.2, panel B). These lipid monolayers or Langmuir films (Langmuir, 1917) can be compressed in two dimensions by barriers while simultaneously monitoring surface pressure π by microbalance thus yielding a compression isotherm. Depositing lipids at air/water interface simplifies model system and some advantages over liposomes are gained. Accordingly, in monolayers surface curvature and lipid composition are precisely controlled, lipid lateral packing can be readily regulated, and area exposed to subphase is exactly known (Brockman, 1999).

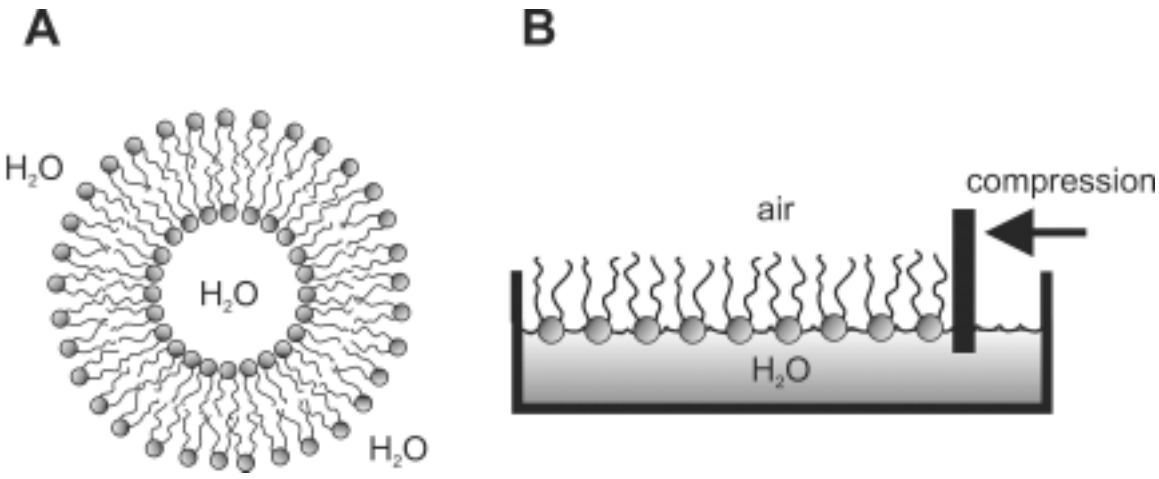

FIGURE 2.2 Panel A, Cross section of a unilamellar liposome. **Panel B**, Schematic illustration of a lipid monolayer on air/water interface.

2.1.3 Overview of the physical properties of lipids

From physical point of view basic structure of biomembranes, i.e. lipid bilayer, can be described as liquid-crystal demonstrating complex phase behavior depending on both temperature (thermotropic transitions) and lipid concentration (lyotropic transitions) (Nagle and Tristram-Nagle, 2000). Lipid phase transitions have been studied extensively by means of various techniques such as differential scanning calorimetry (DSC), X-ray and neutron diffraction, electron microscopy, as well as nuclear magnetic resonance (NMR), infrared, and fluorescence spectroscopy (Kinnunen and Laggner, 1991). Most studied and best understood lipid phase transition involves change from lamellar and ordered gel L_β phase through intermediate rippled gel P_β phase to fluid, liquid crystalline L_α phase. A phase transition is accompanied by a change in enthalpy as rearrangement of molecules requires energy and thus can be observed as a peak in excess specific heat in a DSC heating scan (McElhaney, 1982). This is exemplified by DSC trace of dimyristoylphosphatidylcholine (DMPC) liposomes demonstrating two endothermic peaks at pretransition temperature $T_p \approx 14$ °C and main transition temperature $T_m \approx 24$ °C denoting transition from L_β to P_β phase and from P_β to L_α phase, respectively (Fig. 2.3, panel A).

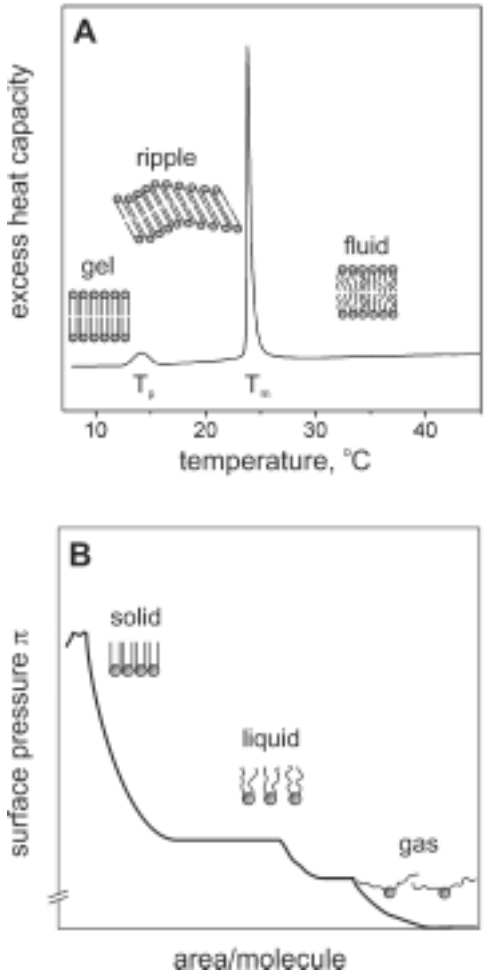

Transition from gel to fluid state, i.e. the main transition, is reflected in properties and structure of lipid bilayer at three levels of molecular organization, viz. at level of (i) lipid acyl chains, (ii) individual lipid molecules, and (iii) supramolecular assembly as a whole. At T_m acyl chains of the lipids melt, i.e. their conformation changes from rather rigid and straight all-*trans* state of the gel phase to more flexible all-*gauche*

FIGURE 2.3 Panel A, A DSC trace for DMPC MLVs with schematic illustrations of ordered gel (L_β) , rippled gel (P_β), and fluid (L_α) phases separated by endothermic peaks denoting pretransition and main transition at temperatures T_p and T_m, respectively. **Panel B**, A schematic representation of compression isotherm of lipid monolayer depicting general structures of gas, liquid, and solid phases.

conformation of the liquid disordered phase (Fig. 2.3, panel A). Augmented freedom of movement of the acyl chains can be observed as expansion of cross-sectional area and, to lesser extent, increment in volume occupied by acyl chains as well as thinning of the membrane thickness (Heimburg, 1998). In keeping with the above both T_m and enthalpy of transition (ΔH) evident as area of the transition peak in DSC trace are elevated with increasing length of fatty-acid chains, while introducing *cis*-double bonds to acyl chains has the opposite effect on these variables. Moreover, diffusion of the individual lipid molecules, including lateral movement in the plane of bilayer, rotation around molecular axis, protrusion in and out of bilayer plane, as well as flip-flop between lipid monolayers, is greatly increased upon exceeding T_m (Mouritsen, 2005). Finally, lipid bilayer is much more elastic in fluid than gel state, and even more so in the gel-fluid co-existence regime of the main transition (Heimburg, 1998; Evans and Kwok, 1982; Needham and Evans, 1988). The exact nature of preceding pretransition from L_β to P_β is a matter of dispute. X-ray studies have shown that in P_β lipid hydration is enhanced compared to L_β phase, bilayer forms periodic membrane ripples, and is organized in two domains with differing membrane thickness (Nagle and Tristram-Nagle, 2000; Sun et al., 1996). As an explanation for the above recent molecular dynamics study suggests complete chain interdigitation in thinner domains while thicker domains would retain gel-like order of the L_β phase (de Vries et al., 2005). Similar lipid phase transitions are observed also in Langmuir monolayers during two-dimensional compression (Fig. 2.3, panel B) though fundamental differences between monomolecular lipid films and bilayers warrant some caution when making conclusions based on this analogy. In brief, as the area per molecule is diminished monolayer proceeds through a sequence of transitions starting from very dilute gaseous phase to liquid expanded phase and liquid condensed phase, and finally, before eventual collapse of monolayer, to very densely packed solid phase demonstrating exponential increase in surface pressure as a response to compression (Kaganer et al., 1999).

Cholesterol is an abundant lipid in eukaryotic biomembranes accounting up to 30-50 mol% of the total lipids in plasma membrane. The steroid structure of cholesterol molecule is rather stiff and smooth favoring gel-like ordered conformation of vicinal lipid acyl chains, but on the other hand its molecular shape is markedly different from other lipids thus disrupting packing order of neighboring phospholipids. Accordingly, to accommodate better into lipid bilayer cholesterol induces so-called liquid-ordered phase which is an intermediate between L_β and L_α phases demonstrating rapid lateral diffusion of lipids similar to fluid bilayers and conformational order of acyl chains resembling that of the gel phase membranes (Mouritsen

and Zuckermann, 2004). Furthermore, incorporation of cholesterol into phospholipid membrane increases thickness of bilayer, reduces its elasticity, and diminishes permeability (Mouritsen and Zuckermann, 2004).

An important feature of lipid membranes is their lateral heterogeneity, i.e. they demonstrate long-range lateral organization. Even lipid membranes consisting of a single constituent, such as above discussed DMPC liposomes, show domain formation in the main phase transition regime when lipid microdomains in gel and fluid phases coexist (Shimshick and McConnell, 1973). Phase separation is more pronounced in mixed lipid membranes and has been visualized in monolayers (Weis, 1991) and giant vesicles (Bagatolli, 2003) by fluorescence microscopy as well as by atomic force microscopy in supported model membranes (Leidy et al., 2002). Driving forces for such lateral segregation are diverse including e.g. dehydration of membrane (Lehtonen and Kinnunen, 1995), electrostatic interactions with macromolecules (Kõiv et al., 1994; Kleinschmidt et al., 1998), and lipid-lipid (Lehtonen et al., 1996) or lipid-protein (Mouritsen and Bloom, 1984) hydrophobic mismatch.

In addition to phase transitions in lamellar geometry lipids undergo transitions between various non-lamellar mesophases (Tate et al., 1991). These transitions relate to effective shapes of lipid molecules (Kinnunen, 1996) that dictate the packing of lipids into different geometries (see section 2.1.1 for details) and can be induced e.g. by varying temperature, headgroup hydration, or ionic strength of the surrounding medium. Different 3-D phases have significant impact on biological membrane processes. For instance so-called cubic mesophases are suggested to be present in a number of cellular membrane structures such as inner mitochondrial membrane, endoplasmic reticulum, and plasma membrane (Landh, 1995) while inverted non-lamellar phases are involved in fusion processes of biomembranes (Kinnunen and Holopainen, 2000) and liposomal transfection discussed in more detail in section 2.3.

2.1.4 Charged lipids

Nearly all lipids have ionic charges in their hydrophilic headgroups. For instance, phospholipids have both negatively charged phosphate and positively charged ammonium moiety in the headgroup and can thus be termed as zwitterions. However, generally only lipids bearing net electric charge are considered as "charged". Even when employing this strict definition for charged lipids they are ubiquitously present in cellular membranes.

Introducing charged lipids into model membranes has profound impact on membrane properties including hydration and thermodynamics, as well as distribution of ions in the vicinity of the surface (Cevc, 1990). Accordingly, acidic phospholipids that bear negative charge in deprotonated form represent means to regulate various biochemical processes e.g. by direct electrostatic interaction with macromolecules, changing physical state of the membrane accommodating the functional protein, or electrostatically attracting substrates into vicinity of an enzyme (Langner and Kubica, 1999; Kinnunen et al., 1994). Furthermore, it was recently described that acidic phospholipids can complex with cationic proteins to form macroscopic fibrous structures with amyloid characteristics (Zhao et al., 2004). Also natural cationic lipids, viz. sphingosine and sleep-inducing lipid oleamide (Cravatt et al., 1995), are found in cells. Sphingosine, a metabolite of sphingolipids abundant in nuclear membrane, has been shown to have a range of interesting effects. Sphingosine affects thermal phase behavior of phospholipid membranes (Kõiv et al., 1993), it avidly interacts with DNA (Kõiv and Kinnunen, 1994; Kinnunen et al., 1993), forms ternary complexes with DNA and histones (Kõiv et al., 1995), and induces lateral ordering into time-averaged superlattices in mixed sphingosine/POPC monolayers (Säily et al., 2003).

Interactions of charged lipid membranes and counterions in surrounding solution are classically described by Gouy-Chapman approximation that simplifies system by treating counterions as point charges and confining membrane charges into infinitely narrow plane (Cevc, 1990). Despite its simplicity Gouy-Chapman theory complies surprisingly well with most experimental results. For instance, the impact of varying protonation and electrostatic screening by NaCl on T_m of acidic phospholipid phosphatidylserine liposomes can rather reliably be explained by Gouy-Chapman approximation (Cevc et al., 1981). More specifically, both increased protonation and electrostatic screening by NaCl elevate T_m because of the diminished Coulombic repulsion between headgroups and subsequent condensation of the bilayer that increases chain-chain interactions and, accordingly, thermal energy required for *trans→gauche* isomerization of the acyl chains. However, there are significant oversimplifications in Gouy-Chapman theory. Notably, it neglects the impact of headgroup hydration and structural changes within membrane, e.g. conformational changes of the lipids (Cevc, 1990). Moreover, since the counterions are treated as point charges their geometry is completely omitted and thus all ions with equal valence produce similar effects. This is in contrast with experimental results including classical experiments by Franz Hofmeister that revealed specificity of the ion effects on proteins and lipids (Kunz et al., 2004a; Kunz et al., 2004b).

2.1.5 Gemini surfactants

Gemini surfactants, or bis-surfactants, (Menger and Littau, 1993) composed of two conventional surfactant molecules whose polar headgroups are connected by a spacer (Fig. 2.4), have acquired widespread interest in colloid and surface chemistry during the last decade. Geminis have almost 100-fold lower critical micellar concentrations (CMCs) and even 1000-fold higher surface activities compared to conventional surfactants with comparable acyl chain length. Importantly, chemical structure of geminis can be modified relatively easily and molecules with specifically designed properties can be synthesized to meet the requirements of various applications ranging from solubilization processes to disinfection (Menger and Keiper, 2000). By systemically altering the gemini structure the effective shape of surfactants and, accordingly, also the topology of 3-D assemblies formed by them can be controlled thus making geminis ideal molecules for applications requiring precisely designed self-assembly, such as liposomal gene delivery (Kirby et al., 2003). In order to utilize the full potential of gemini surfactants principles governing their phase behavior have been characterized by techniques such as DSC (Menger and Mbadugha, 2001; Ryhänen et al., 2002), Langmuir monolayer (Sumida et al., 1996), NMR (Luchetti and Mancini, 2000), as well as electron microscopy (Sommerdijk et al., 1997; Menger et al., 2000; Menger and Peresypkin, 2001). Yet, after a decade of research on geminis understanding on their complex phase behavior is still rudimentary compared to phospholipids studied extensively for half a century.

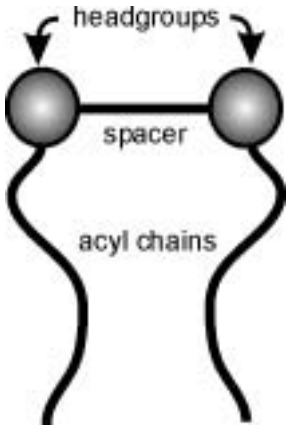

FIGURE 2.4 General structure of gemini surfactants.

2.2 GENE TRANSFER VECTORS – AN OVERVIEW

Ever since discovery of the basic structure and function of the human genome utilization of gene products as a remedy for both inherited and acquired diseases has been an important goal for biomedical research. The "great genome project" has provided vast amount of detailed information about human genome and simultaneously identified plethora of genes with therapeutic potential. Yet, mere identification and isolation of the therapeutic gene is not nearly sufficient for successful gene therapy. Reliable delivery of the genetic material into eukaryotic cells followed by adequate expression of the desired gene is a bottleneck for gene transfer even in cell cultures. Delivery is even more problematic *in vivo* where targeting and safety of the gene vectors as well as rapid elimination from circulation present additional challenges for successful gene transfer. Accordingly, intensive research efforts have focused to create safe, efficient, and reliable strategies to convey nucleic acids into eukaryotic cells.

Viruses represent natural first choice for gene transfer as their transfection efficiency is streamlined by long evolutionary history and is still unsurpassed by their synthetic counterparts (Thomas et al., 2003). First gene therapy trials showing real therapeutic benefit have been done using viral gene transfer, of which probably the most important is the sustained treatment of nine children with X-linked severe combined immunodeficiency (SCID) (Cavazzana-Calvo et al., 2000; Hacein-Bey-Abina et al., 2002). However, viral gene delivery is by no means an ideal choice because of multiple drawbacks including cytotoxicity, immunological responses, possibility of insertional mutagenesis, and limitations of large-scale production (Glover et al., 2005). Recent reports have raised serious questions about the safety of the viral vectors as a patient died of systemic inflammatory reaction after adenoviral gene transfer (Raper et al., 2003) and three out of nine children cured from SCID developed leukemia due to integration of retrovirus vector in the vicinity of a proto-oncogene promoter (Hacein-Bey-Abina et al., 2003a; Hacein-Bey-Abina et al., 2003b). Shortcomings of viral gene transfer emphasize the need for alternative methods with improved safety and adequate gene transfer efficiency (Glover et al., 2005). So-called physical transfection methods promote entry of nucleic acids into cells by disrupting plasma membrane by electric shock ("electroporation") or osmotic stress, or alternatively DNA is directly injected or shot on a coated microparticle into cells. As the utilization of the latter methods is restricted for topical or *ex vivo* applications, synthetic vectors based on complexation of anionic nucleic acid either

with cationic liposomes (Felgner et al., 1987) or cationic polymers (De Smedt et al., 2000) are considered more promising alternatives for viral transfection (Glover et al., 2005).

2.2.1 Liposomes in transfection

Cationic liposome-DNA complex was the first non-viral transfection vector described (Felgner et al., 1987), and has become the most popular transfection method *in vitro*. These so-called "lipoplexes" (for nomenclature see Felgner et al., 1997) provide promising alternative for viral transfection as they lack the biohazards of the viruses. Liposomes are known to be safe and reliable drug carriers *in vivo* and are approved for clinical use as drug delivery systems (Allen, 1997; Allen, 1998; Peñate Medina et al., 2004). Moreover, lipoplexes are easy to prepare compared to viral constructs: positively charged liposomes and negatively charged DNA complex spontaneously in aqueous solution mainly due to electrostatic interaction, while also counterion release (Wagner et al., 2000) and hydrophobic interaction (Kikuchi and Carmona-Ribeiro, 2000; Matulis et al., 2002) contribute. Cationic liposomes can be complexed also with other anionic polyelectrolytes than DNA thus broadening their usage to deliver anti-sense oligonucleotides (Meyer et al., 1998) or small inhibitory RNA (siRNA) (Soutschek et al., 2004) to modify gene expression in eukaryotic cells. Lipoplexes can be further modified to improve their properties as *in vivo* gene vectors by anchoring functional molecules via hydrophobic moiety on their surface. For instance, lipoplexes with molecules such as transferrin receptor antibodies (Shi et al., 2001) or folate (Reddy et al., 2002) have been constructed to target them into brain tissue and folate receptor-expressing tumor cells, respectively.

2.3 LIPOFECTION – BARRIERS AND CARRIERS

In order to be expressed in a eukaryotic cell foreign DNA has to reach the nucleus where transcription machinery is located. Accordingly, way to successful lipofection proceeds through barriers posed by extracellular environment and intracellular structures (Zuhorn and Hoekstra, 2002; Zabner et al., 1995; Simoes et al., 1999; Belting et al., 2005). Overcoming these barriers by cunning lipoplex design based on knowledge about structure-function relationship of lipoplexes is the cornerstone of research aiming to enhance lipofection

efficiency (Zuhorn and Hoekstra, 2002; Chesnoy and Huang, 2000; Elouahabi and Ruysschaert, 2005). In this section barriers to lipofection as well as structural and functional features helping lipoplexes to cross them are briefly discussed.

2.3.1 Extracellular barriers

Environment outside the cell is hostile for lipofection both *in vitro* and *in vivo*. When complexed with cationic liposomes DNA is fairly well protected from action of degrading enzymes (Gershon et al., 1993; Xu and Szoka, 1996) and nucleases (Bhattacharya and Mandal, 1998) as it is condensed and enveloped by a lipid layer (Bloomfield, 1996; 1998; Sternberg et al., 1994). However, cell culture medium contains number of serum proteins, e.g. albumin, lipoproteins, and macroglobulins, that could interfere with interaction between lipoplexes and cells thus causing less efficient transfection (Zelphati et al., 1998; Tandia et al., 2003). Interaction with serum components prior to encounter with cells has been shown to influence also lipoplex structure diverting its intracellular processing (Zuhorn et al., 2002b). Serum effects on lipofection efficiency seem to be dependent on chemical structure of cationic lipid, liposome formulation, and cationic lipid/DNA ratio of the lipoplexes (Zelphati et al., 1998; Simberg et al., 2003; Tandia et al., 2005) but detailed understanding of lipoplex-serum interactions is still incomplete.

In vivo the number of extracellular barriers for liposomal delivery of a transgene is multiplied as many physiological processes, such as complement activation and function of reticulo-endothelial system rapidly clear lipoplexes from the circulation (Bally et al., 1999; Dass, 2004). Targeting lipoplexes into desired tissues instead of nonspecific transfection in liver or lungs (Parker et al., 1997; Niven et al., 1998) presents an additional challenge for *in vivo* lipofection. The most popular strategy to prolong circulation times of lipoplexes and simultaneously incorporate targeting molecules onto surface of the gene delivery complex is coating of lipoplexes by lipids with conjugated PEG moiety (Zhang et al., 1999; Tam et al., 2000). Major drawback of these "stabilized plasmid-lipid particles" is their low transfection efficiency even *in vitro* due to stabilizing PEG-coating. However, lipofection efficiency could be at least partly recovered by introducing positively charged moiety to distal end of the PEG chain (Chen et al., 2000).

2.3.2 The plasma membrane

Plasma membrane is the natural permeability barrier of a eukaryotic cell that lipoplex has to penetrate to reach the intracellular space. Association of lipoplex onto cell surface is driven by net positive charge of lipoplex, most likely via electrostatic binding to proteoglycans of the outer leaflet of plasma membrane (Mislick and Baldeschwieler, 1996; Reimer et al., 1997; Arima et al., 1997; Mounkes et al., 1998). Importantly, also cytotoxicity of the lipoplex is related to charge ratio of lipoplex and may ensue when cationic amphiphiles mix with lipids of cellular membranes (Zuhorn and Hoekstra, 2002; Dass, 2004). Initially it was proposed that internalization of lipoplexes proceeds through direct fusion with plasma membrane (Felgner et al., 1987). Yet, at present wealth of data indicates that endocytosis is the most important internalization route for lipoplexes (Zabner et al., 1995; Wrobel and Collins, 1995). More specifically, it has been suggested that small lipoplexes with diameter < 200 nm enter cells via clathrin-dependent endocytosis while larger complexes prefer caveolae-mediated route (Rejman et al., 2004), and it has been further shown that it is the former pathway leading to more efficient lipofection (Zuhorn et al., 2002a). However, considering great variability in chemical structures of cationic lipids and diversity of eukaryotic cells it is likely that details of endocytotic pathway may vary markedly depending on the cell type (Elouahabi and Ruysschaert, 2005).

2.3.3 Cytoplasm and endosomal escape

Internalized plasmid DNA has to find its way to nucleus through cytoplasm. After endocytosis the cargo entrapped in liposomes goes to endosomes and eventually ends up in lysosomes whose environment is detrimental for DNA (Straubinger et al., 1983; Friend et al., 1996). Accordingly, escape of DNA from the endosomal compartment is absolutely required for successful gene delivery. It has been shown that anionic lipids present in endosomal membranes readily mix with cationic lipids of lipoplexes resulting in interlipidic ion-pairing and subsequent release of nucleic acid from the complex (Kinnunen et al., 1993; Bhattacharya and Mandal, 1998; Zelphati and Szoka, 1996). Moreover, formation of membrane destabilizing hexagonal inverted (H_{II}) instead of lamellar (L_{α}) phase (Fig. 2.5) correlates with efficient lipofection (Mok and Cullis, 1997; Koltover et al., 1998). Consistent with the above most efficient lipoplex formulations contain H_{II}-phase forming lipids, such as dioleylphosphatidylethanolamine (DOPE) (Farhood et al., 1995) or diacylglycerol (DAG) (Paukku et al., 1997), and cationic lipids with effective shape favoring H_{II}-phase are more effective in lipofection than similar molecules preferring lamellar packing (Smisterova et al., 2001). Accordingly, endosomal escape is likely to be a result from destabilizing action of

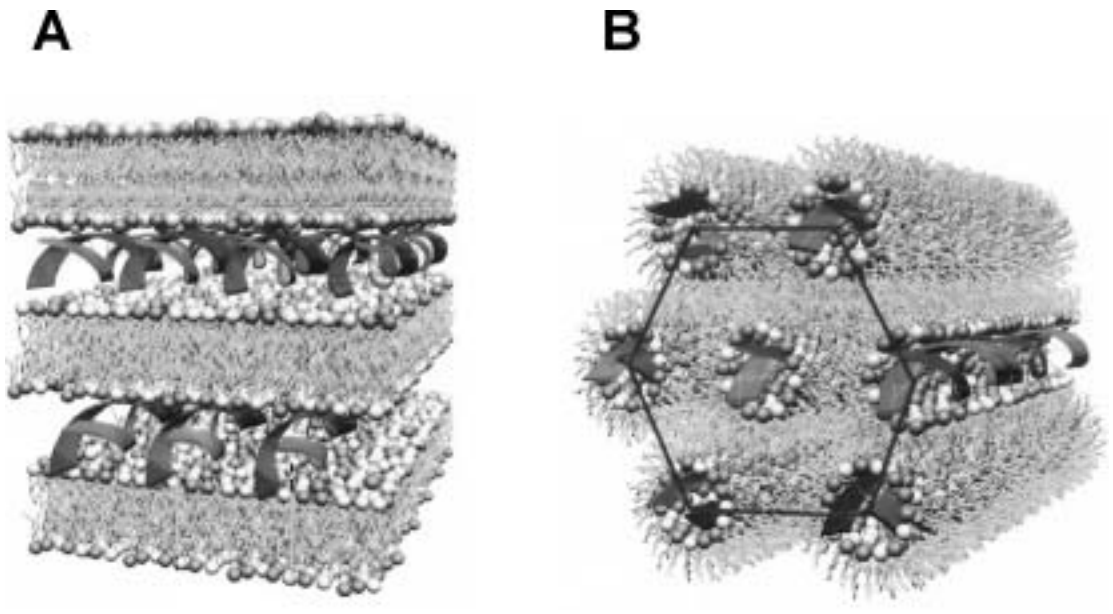

FIGURE 2.5 Schematic illustration of lamellar L_{α} (**Panel A**) and inverted hexagonal H_{II} (**Panel B**) phases of lipoplexes. Ribbons depict DNA complexed with cationic lipid membrane. Adapted from Koltover et al., 1998.

lipids of the lipoplex on the endosomal membrane. Interestingly, when mixed in nearly isoelectric stoichiometry pairing of cationic and anionic lipid induces lamellar to hexagonal phase transition although both of the lipids adopt lamellar phase in isolation (Lewis and McElhaney, 2000), suggesting that also mixing of anionic and cationic lipids could induce endosomal membrane destabilization by promoting H_{II} phase (Hafez et al., 2001). To enhance endosomal escape lipoplexes have been designed that disrupt endosomal membrane and release DNA in the low pH of endosomes by virtue of pH dependent transitions (Budker et al., 1996; Fielden et al., 2001). However, despite promising preliminary results pH-sensitive lipoplexes have thus far demonstrated only limited enhancement of lipofection efficiency in practice.

2.3.4 The nuclear membrane

Nuclear membrane is the final and probably the most challenging barrier for lipofection. Data on nuclear entry of the plasmid DNA is somewhat controversial but some basic principles are known. DNA complexed with cationic lipid is not expressed if it is directly injected into nucleus thus suggesting that DNA has to be released from lipoplex somewhere in the cytoplasm, e.g. after fusion with intracellular membrane structures (Zabner et al., 1995; Pollard et al., 1998; El Ouahabi et al., 1999). Yet, the half-life of free DNA in the cytoplasm is only 50-90 min (Lechardeur et al., 1999) setting rather narrow time-window for nuclear entry of plasmid after dissociation from the lipoplex. A close correlation between onset of transgene expression and mitosis in synchronized cell cultures has been established (Mortimer et al., 1999; Tseng et al., 1999) revealing fragmentation of nuclear membrane during mitosis to facilitate DNA entry into nucleus. However, also non-dividing cells can be transfected by lipoplexes albeit with lesser efficiency indicating that mitosis is not absolutely required for nuclear entry (Zuhorn and Hoekstra, 2002). Injection of highly condensed DNA complexed with polyethyleneimine (PEI) into cytoplasm results in efficient transgene expression suggesting that properly packed DNA particles can access the nucleus (Pollard et al., 1998; Suh et al., 2003). Accordingly, condensation and subsequent conformational changes of DNA induced by cationic liposomes could be important not only for protection of DNA in extracellular space but also for nuclear entry and transcriptional activity of the nucleic acid (Bloomfield, 1996; Akao et al., 1996; Gelbart et al., 2000; Braun et al., 2003).

3. OUTLINE OF THE PRESENT STUDY

Cationic lipids have gained widespread interest after their usage as non-viral *in vitro* transfection vectors was introduced. Despite intensive research knowledge about fundamental biochemical and -physical parameters determining transfection efficiency of cationic lipid-DNA complexes is still incomplete. This lack of understanding hampers rational design of better lipofection systems and utilization of lipoplexes in clinical applications. In line with the above major aims of the present study were:

(*i*) To determine impact of the surface charge density on lipofection efficiency of DHAB/DMPC liposomes complexed with EGFP coding plasmid.

(*ii*) To elucidate the effect of surface charge density on biophysical and -chemical parameters of DHAB/DMPC liposomes.

(*iii*) To compare findings from transfection and biophysical studies in an attempt to further our understanding about structure-function relationship of lipoplexes.

(*iv*) To investigate self-assembly of positively charged lipid membranes under various conditions including in high ionic strength medium and as a complex with highly charged polyanion DNA.

4. MATERIALS AND METHODS

4.1 MATERIALS

Calf thymus DNA, DMPC, POPC, Hepes, ethidium bromide, and EDTA were purchased from Sigma. DPH-PC was from Molecular Probes (Eugene, OR, USA), sodium chloride from J. T. Baker (Deventer, Holland), and DHAB from Fluka. Synthesis of the gemini surfactant (2R,3S)-2,3-dimethoxy-1,4-bis(N-hexadecyl-N,N-dimethylammonium)butane dibromide (M-1, Fig. 4.1) is described in detail in publication IV. The purity of M-1 was verified by elemental analysis and electrospray mass spectroscopy while for other lipids thin-layer chromatography on silicic acid coated plates (Merck, Darmstadt, Germany) was utilized. Concentrations of DMPC, POPC, DHAB, and M-1 were determined gravimetrically using a high precision electrobalance (Cahn, Cerritos, CA, USA), while concentration of DPH-PC was determined by absorption at 355 nm (ε = 80,000 $cm^{-1}M^{-1}$). DNA concentrations (expressed in mM basepairs) were determined by absorbance at 260 nm (ε = 6,600 $cm^{-1}M^{-1}$). The 260/280 ratio of the calf thymus DNA was approx. 1.9. Freshly deionized filtered water (Milli RO/Milli Q, Millipore Inc., Jaffrey, NH, USA) was used in all experiments.

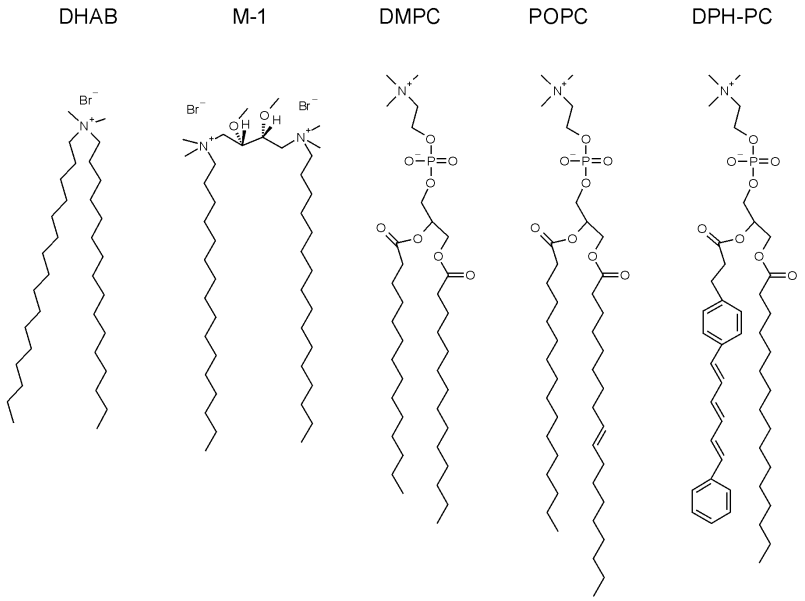

FIGURE 4.1 Chemical structures of the amphiphiles used in this study.

4.2 METHODS

4.2.1 Vesicle preparation (I, II, and IV)

Multilamellar vesicles (MLVs) were prepared by mixing appropriate amounts of the lipid stock solutions in dry chloroform to obtain the desired compositions after which the solvent was evaporated under a stream of nitrogen. For removal of residual solvent the samples were further maintained under high vacuum for at least 2 hrs. The resulting dry lipid films were then hydrated with indicated buffer and thereafter incubated for 30 min at approx. 60 ^{o}C, i.e. above the temperatures of the transition endotherms of the lipid components and their mixtures. To obtain large unilamellar vesicles (LUVs) the hydrated lipid dispersions were vortexed vigorously and then extruded with a LiposoFast small volume homogenizer (Avestin, Ottawa, Canada) by subjecting to 19 passes through polycarbonate filter (100 nm pore size, Nucleopore, Pleasanton, CA, USA). LUVs with diameters of approx. 100 - 115 nm are produced by this method (MacDonald et al., 1991; Wiedmer et al., 2001). Unless otherwise stated the liposomes were kept on an ice water bath for at least 12 hrs before their use. Importantly, to avoid interference with fluorescence spectroscopy resulting from light scattering due to varying lipid concentrations X_{DHAB} was varied these measurements (as well as in DSC experiments) by altering both the amount of DHAB and DMPC while keeping total lipid concentration constant. In the transfection experiments the total cationic charge (i.e. the amount of DHAB) was maintained constant for each CL/DNA ratio and X_{DHAB} was varied by altering the amount of DMPC in the liposomes.

4.2.2 Transfection experiments (I)

The pEGFP-N1 expression vector (Clontech, Palo Alto, CA, USA) consisting of the transcriptional regulatory domain of cytomegalo virus preceding the enhanced green fluorescent protein (EGFP) gene was used in all experiments and prepared using QIAGEN Plasmid Maxi Kit (Qiagen GmbH, Hilden, Germany). Specific restriction endonuclease digestions confirmed the identity of the plasmid.

Transfection efficiencies were measured using COS-1 cells, derived from simian kidney cell line CV-1 transformed with a mutant simian virus 40 (Gluzman, 1981). Cells were grown in Dulbecco's modified Eagle's medium with 10% fetal calf serum (DMEM-10) on 24-well plastic cell culture plates in an incubator with an atmosphere of 5% CO_2 in air. Two different kinds of liposome-DNA complexes were made. Accordingly, either MLVs or LUVs, as indicated, were first formed and the plasmid was then added to these liposome solutions. MLVs and LUVs were prepared as described above. These preformed liposomes were then allowed to complex with DNA by adding the indicated amounts of pEGFP-N1 plasmid at 23 ^{o}C in 0.6 ml of serum free Dulbecco's modified Eagle's medium (DMEM-SF), followed by an incubation for 15 min at 23 ^{o}C. Before transfection the total volume of the suspensions containing liposome-plasmid complexes was adjusted to 0.9 ml with DMEM-SF. DMEM-10 was removed from the wells of just confluent 24-well cell culture plates and the liposome-plasmid complexes were added to three separate wells, 0.3 ml to each. After a 6-hour incubation at 37 ^{o}C the transfection mixture was replaced by DMEM-10. Transfection efficiency was determined after 65 hrs of incubation at 37 ^{o}C by measuring the fluorescence intensity of EGFP using SPECTRAFluor Plus fluorescence reader (Tecan AG, Hombrechtikon, Switzerland) with emission and excitation wavelengths set at 485 and 510 nm, respectively. The background measured for non-transfected cells serving as controls was subtracted from the values recorded for the transfected cells.

4.2.3 Cytotoxicity assay (I)

Cytotoxicity was assessed by Trypan Blue (Invitrogen, San Diego, CA, USA) exclusion. Cells were cultured on 24-well culture plates in DMEM-10 and subsequently incubated at 37 ^{o}C for 6 hrs with lipoplexes with the indicated compositions, after which the transfection mixture was replaced by DMEM-10 and the incubation continued for further 24 hrs. Subsequently, cells were detached from the wells by trypsinization and resuspended in 1 ml of DMEM-SF. An aliquot of 50 µl of the resulting cell suspension was mixed with 50 µl of 0.4% Trypan Blue and incubated at ambient temperature (approx. 23 ^{o}C) for 5 min. The amount of non-viable cells was determined by counting the stained cells with a hemocytometer.

4.2.4 Ethidium bromide intercalation assay (I)

Fluorescence emission spectra of ethidium bromide in the 520-700 nm region were recorded with a Perkin-Elmer LS 50B spectrofluorometer with excitation at 500 nm. In brief, 1.8 ml's of 16 μM EtBr was first applied into a magnetically stirred four-window quartz cuvette thermostated at 37 ^{o}C after which calf thymus DNA was added to yield a final concentration of 34 μM (expressed in basepairs). Subsequently, LUVs of the given compositions were included to achieve the indicated molar ratios. Emission spectra were measured 5 min after the addition of liposomes.

4.2.5 Static light scattering (I)

Static light scattering due to the formation of complexes by the cationic liposomes and DNA was measured with a Perkin-Elmer LS 50B spectrofluorometer with both excitation and emission monochromators set at 500 nm. Two ml's of 50 μM liposome solution of the indicated composition was placed into a magnetically stirred four-window quartz cuvette thermostated at 37 ^{o}C. LUVs and DNA were mixed at the stated molar ratios. Scattering intensities were measured 5 min after the addition of DNA to the indicated concentrations and remained constant after this period.

4.2.6 Differential scanning calorimetry (II)

After hydration MLVs were vortexed and immediately loaded without prior incubation on ice into the calorimeter cuvette (final concentration 1 mM). A VP-DSC microcalorimeter (Microcal Inc., Northampton, MA, USA) was operated at a heating rate of 0.5 degrees per minute. Data were analyzed using the routines of the software provided by the instrument manufacturer.

4.2.7 Monolayer measurements (III and IV)

A computer controlled Langmuir-type film balance (μThroughS (III) or MicroThrough XS (IV), Kibron Inc., Helsinki, Finland) was used to record compression isotherms (π-A). All glassware used was rinsed thoroughly with ethanol and water. The amphiphile was mixed in chloroform and spread in this solvent onto the surface of 14 ml of indicated buffer at approx. 21°C. To ensure complete evaporation of the solvents the films were allowed to settle for 4 min prior to the recording of the π-A isotherms. The monolayers were compressed by two symmetrically approaching barriers at a rate of < 4 $Å^2$/molecule/min, so as to allow for the reorientation and relaxation of the lipids in the course of the compression. Surface pressure was measured by the Wilhelmy technique with a small diameter alloy probe placed in the air/water interface and hanging from a high sensitivity microbalance (KBN 502, Kibron Inc.). Surface pressure π is defined as

$$\pi = \gamma_0 - \gamma$$

where γ_0 is the surface tension of the air/buffer interface and γ is the value for surface tension in the presence of a lipid monolayer compressed at varying packing densities. $A_{lift\text{-}off}$ (IV) was determined as the area at which the surface pressure begins to deviate from the baseline thus reflecting the packing conditions in monolayers at low surface pressures.

4.2.8 Fluorescence spectroscopy and static light scattering (II)

The fluorescence spectra, anisotropy, and static light scattering data were collected using Varian Cary Eclipse equipped with a Peltier thermostated cuvette compartment containing four cuvettes and a temperature probe immersed in a cuvette filled with Millipore water. For fluorescence experiments DPH-PC was added to vesicles so as to yield a 1:500 molar ratio of the probe to lipid ($X_{DPH\text{-}PC}$ = 0.002). After hydration vesicles were vortexed and immediately (without incubation on ice) diluted in 5 mM Hepes, 0.1 mM EDTA, pH 7.4 to final concentration of 50 μM. When indicated NaCl was included in buffer used for dilution of the vesicles. Changes in membrane acyl chain order were assessed by measuring the steady state anisotropy r for DPH-PC (Lakowicz et al., 1979a; Lakowicz et al., 1979b). In brief, the fluorophore was excited at 345 nm while anisotropy values were recorded at 450 nm with

polarizers in the excitation and emission pathways. Corresponding bandpasses were 5 and 10 nm. Anisotropy is defined by (Lakowicz, 1999):

$$r = \frac{I_{\parallel} - I_{\perp}}{I_{\parallel} + 2I_{\perp}},$$

where $I_{\parallel}$ and $I_{\perp}$ are the intensities of fluorescence emission recorded with emission polarizer oriented parallel and perpendicular, respectively, to the direction of vertically polarized excitation. G-factor, the ratio of sensitivities of the instrument for vertically and horizontally polarized light, was determined before every measurement and was used to correct the anisotropy values (Lakowicz, 1999). Emission spectra were collected in the range 370 – 550 nm as above except without using polarizers in the optical pathways. Static light scattering for DHAB/DMPC/DPH-PC liposomes was measured at an angle of 90°, incident wavelength was set as 550 nm, and the integrated intensity of scattered light from range 540 to 560 nm was calculated.

4.2.9 Fourier transform infrared spectroscopy (II)

Appropriate amounts of DMPC and DHAB were mixed and dispersed into Millipore water so as to reach a total lipid concentration of 10 mg/ml. Subsequently, the solution was incubated for 30 min at 60 ^{o}C and vigorously vortexed every 10 min after which the solution was sonicated in a bath type sonicator for 20 min. Approx. 1.5 ml of the resulting vesicle solution was loaded on a zinc selenide attenuated total reflectance (ATR) crystal that was temperature controlled by an external circulating water bath (ThermoHaake, Karlsruhe, Germany). Vesicles were allowed to deposit on the crystal surface and the temperature to stabilize the sample was kept at each defined temperature for approx. 15 min before recording spectra. The latter were collected by Bruker EQUINOX 55 spectrometer (Bruker, Karlsruhe, Germany) using mercury-cadmium-telluride detector. The sample compartment was purged with dry air generated by an adsorber (Zander, Essen, Germany). A total of 1024 interferograms were co-added to yield each spectrum and data were analyzed using dedicated software (OPUS) provided by the instrument manufacturer. The resolution of the FTIR spectra collected was 4 cm^{-1} and the frequencies of the IR bands were determined by a routine of OPUS software utilizing second derivative.

4.2.10 Optical microscopy (IV)

An inverted microscope with differential interference optics (Olympus IX-70, Olympus, Japan) and with LCPlanFl 20x/0.40 objective was used for optical microscopy. The images were obtained using a digital camera (Canon D10) attached to the camera port of the microscope. Surfactant suspension (1.5 ml) with the indicated [NaCl] was applied into a chamber with quartz glass bottom. This chamber was heated from 24 °C to 50 °C within approx. 50 min by a Peltier thermal microscopy stage (TS-4, Physitemp, Clifton, NJ, USA) and temperature in the solution was monitored by an immersed probe (Omega, Stamford, CT, USA).

5. RESULTS

5.1 INTERACTIONS OF DHAB/DMPC LIPOSOMES WITH DNA AND CULTURED CELLS (I)

5.1.1 Transfection experiments

In the first series of experiments plasmid DNA was added to MLV solution. The transfection efficiency of the resulting lipoplexes was dependent on X_{DHAB} (Fig. 5.1, panel A). In brief, liposomes with $X_{DHAB} \leq 0.25$ were ineffective or only weakly efficient in transfection. However, a dramatic increase in transfection efficiency followed as X_{DHAB} was increased to 0.50, after which further increasing X_{DHAB} towards neat DHAB liposomes caused a minor decrement in the expression levels. Importantly, these changes cannot be explained by an increment in the total amount of plasmid DNA since it was maintained constant for each CL/DNA ratio (charge of the cationic lipid/negative charge of DNA) studied (i.e. X_{DHAB} was varied by altering the amount of DMPC in the liposomes). Different CL/DNA ratios were achieved by varying the amount of the plasmid

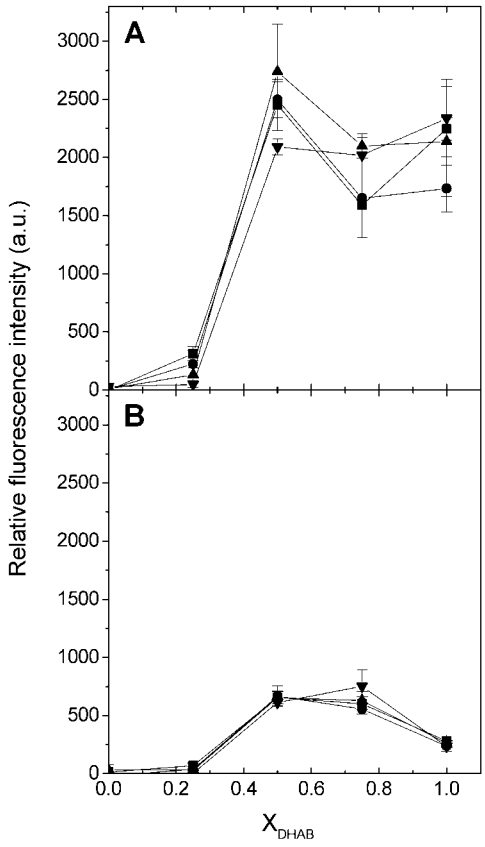

FIGURE 5.1 Comparison of the transfection efficiencies of pEGFP-N1 plasmid in COS-1 cells added to MLVs (**panel A**) or LUVs (**panel B**), illustrated as a function of X_{DHAB}. CL/DNA ratios in the lipoplexes were 0.25 (■), 0.5 (●), 1.0 (▲), and 1.5 (▼). The error bars represent standard error of mean calculated from at least three separate experiments. See Materials and Methods for further details.

DNA (6.0 nmol, 3.0 nmol, 1.5 nmol, and 1.0 nmol, corresponding to CL/DNA ratios of 0.25, 0.5, 1.0, and 1.5), while the amount of cationic charge was kept constant. Variation of CL/DNA between 0.25 and 1.5 had an insignificant impact on the transfection efficiency of DHAB/DMPC MLVs, when $X_{DHAB} \geq 0.50$. The expression levels achieved in our experiments by DHAB/DMPC MLVs at $X_{DHAB} \geq 0.50$ were comparable or higher than those obtained with the commercial cationic liposome vector Lipofectin™ (data not shown).

To allow for comparison of the transfection efficiencies with the physicochemical data on the liposomes we also measured the expression levels using LUVs with the subsequently added plasmid (Fig. 5.1, panel B). In keeping with the results obtained with MLVs (Fig. 5.1, panel A), LUVs having X_{DHAB} between 0.50 and 0.75 gave the highest expression levels. Yet, in accordance with earlier studies (Ross et al., 1998; Ross and Hui, 1999; Zuidam et al., 1999) MLVs were more efficient in transfection than LUVs with similar composition.

The observed dependence of the transfection efficiency of the lipoplexes on X_{DHAB} could be due to the varying cytotoxities of the lipoplexes. To examine this possibility the cytotoxicities of DHAB/DMPC MLVs complexed with the plasmid (CL/DNA = 0.5) were determined as a function of X_{DHAB} by Trypan Blue exclusion. The percentage of non-viable cells as a function of X_{DHAB} revealed only minor differences (Fig. 5.2) and thus we may conclude that differences in transfection efficiencies are not due to cytotoxicity.

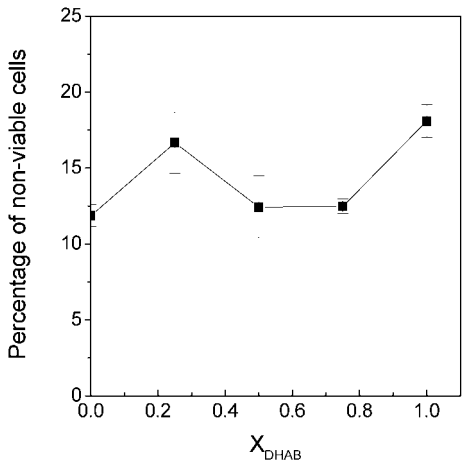

FIGURE 5.2 Cytotoxicity of DHAB/DMPC liposomes complexed with pEGFP-N1 plasmid, determined by Trypan Blue exclusion and expressed as percentage of non-viable cells as function of X_{DHAB}. CL/DNA ratio was 0.5 and the error bars represent standard error of mean calculated from at least three experiments.

5.1.2 DNA condensation induced by DHAB/DMPC LUVs

Static light scattering was utilized to investigate complexation between DHAB/DMPC LUVs and CT-DNA. While neat DMPC LUVs as well as liposomes without DNA scattered only weakly markedly augmented scattering was measured upon addition of DNA to binary DHAB/DMPC liposomes. Scattering intensity did depend on X_{DHAB} (Fig. 5.3). In brief, values for scattering first increased slowly until $X_{DHAB} = 0.50$ and upon exceeding this X_{DHAB} amount of scattered light increased drastically, suggesting formation of more dense complexes and possibly also condensation of DNA (Bloomfield, 1996). After maximum at $X_{DHAB} = 0.6$ a steady decrement in scattering was measured. Liposomes with $X_{DHAB} > 0.75$ showed tendency for precipitation in the presence of DNA, providing a plausible explanation for diminished light scattering.

To verify whether the above observations from light scattering experiments were indeed due to DNA condensation ethidium bromide (EtBr) intercalation assay was employed. Ethidium bromide is a fluorophore whose emission intensity is approximately 10-fold higher when intercalated between the bases of DNA compared to its fluorescence in water (Lakowicz, 1999). During condensation of DNA varying amounts of EtBr are expelled from DNA into the aqueous phase evident as a decrease in fluorescence emission intensity (Bhattacharya and Mandal, 1998; Cain et al., 1978; Geall et al., 1999). The normalized emission intensity of DNA bound EtBr at 590 nm as a function of lipid concentration exhibited two different patterns depending on X_{DHAB} (Fig. 5.4). LUVs with $X_{DHAB} \leq 0.50$ caused only a minor decrement in EtBr emission (approx. 15%), which is likely to result from augmented scattering due to complexation of liposomes with DNA (Fig. 5.3). However, liposomes with $X_{DHAB} > 0.50$ caused a pronounced quenching of emission intensity (maximally by approx. 47%), thus suggesting condensation of DNA by these liposomes. Importantly, the effect was not dependent on the

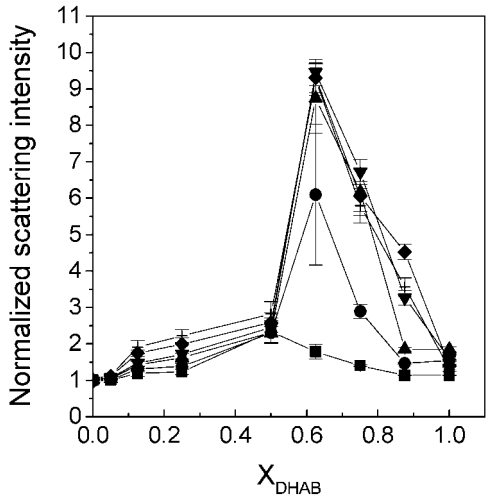

FIGURE 5.3 The static light scattering of liposome-DNA complexes as a function of X_{DHAB}. DNA concentration was 0.5 (■), 1.5 (●), 2.5 (▲), 5.0 (▼), 10.0 (◆), and 15.0 μM (+). Temperature was maintained at 37 °C. Buffer was 5 mM Hepes, 0.1 mM EDTA, pH 7.4 and total concentration of lipid was 50 μM. The error bars represent standard error of mean calculated from at least three experiments.

total amount of cationic charge present since the liposomes with X_{DHAB} = 0.75 and 1.00 show similar behavior despite significant difference in the total amount of cationic surfactant.

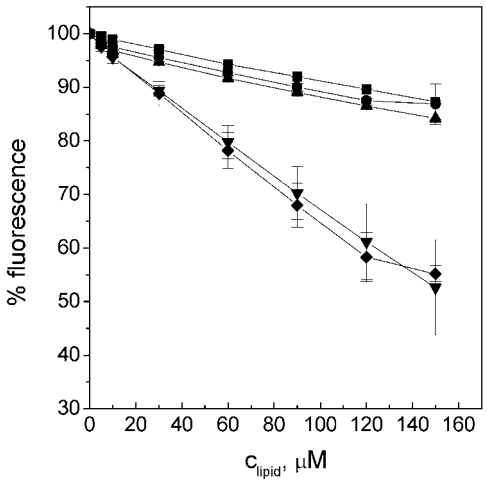

FIGURE 5.4 Normalized fluorescence emission intensity of DNA associated EtBr at 590 nm as a function of lipid concentration. X_{DHAB} = 0.00 (■), 0.25 (●), 0.50 (▲), 0.75 (▼), and 1.00 (◆). Temperature was maintained at 37 ^{o}C. Buffer was 5 mM Hepes, 0.1 mM EDTA, pH 7.4. Total concentrations of DNA and EtBr were 34 μM (in basepairs) and 16 μM, respectively. The error bars represent standard error of mean calculated from at least three experiments.

5.2 IMPACT OF SURFACE CHARGE DENSITY ON DHAB/DMPC MEMBRANES (II, III)

5.2.1 Thermal phase behavior of DHAB/DMPC liposomes

DSC traces recorded for binary DHAB/DMPC MLVs with varying X_{DHAB} are shown in Figure 5.5. To demonstrate the impact of X_{DHAB} on thermal phase behavior of these liposomes main transition temperatures (T_m) were determined both from DSC and fluorescence spectroscopy data (Fig. 5.6, panel A). In the latter experiments fluorescence anisotropy r of DPH-PC (Lakowicz et al., 1979a; Lakowicz et al., 1979b) was measured for DHAB/DMPC vesicles with varying X_{DHAB} in the temperature range of 10 – 50 °C. In the course of the main phase transition the acyl chains become more mobile, evident as a decrease in r centered at T_m. Thus minima for the first derivatives dr/dT yield an approximation for T_m. If the first derivative of the raw data was ambiguously defined a visually acceptable polynomial fit was used for analysis. Boundaries of the phase diagram obtained by both methods gave values for T_m that are consistent with each other (Fig. 5.6, panel A). In brief, T_m of neat DMPC vesicles was 23.2 °C determined by DPH-PC fluorescence and 23.7 °C determined by DSC. As X_{DHAB} was increased T_m progressively rose to a maximum of 42.7 °C (42.1 °C by DSC) at X_{DHAB} = 0.4. At X_{DHAB} > 0.4 the value for T_m decreased until at $X_{DHAB} \geq 0.7$ a plateau at approx. 28 °C was evident. Neat DHAB vesicles demonstrated somewhat higher T_m (T_m = 33.8 °C by DPH-PC fluorescence and 29.4 °C by DSC) compared to vesicles with X_{DHAB} = 0.9,

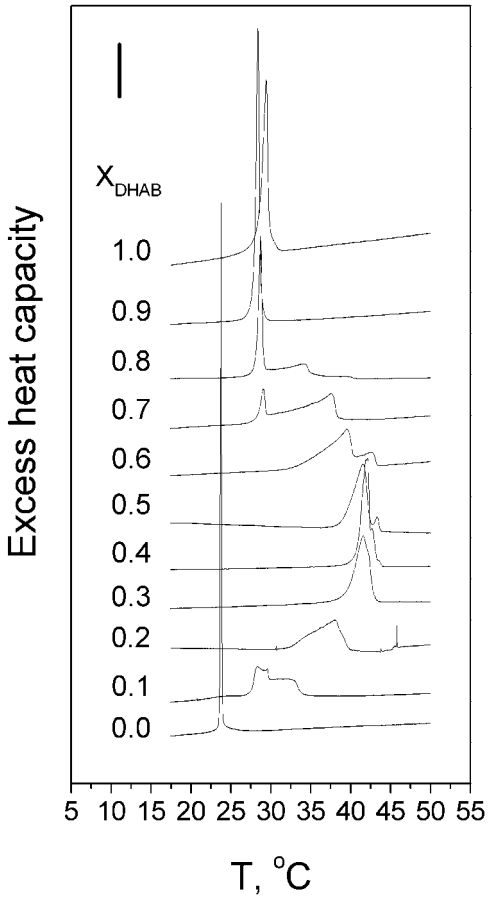

FIGURE 5.5 DSC traces of DHAB/DMPC vesicles with indicated mole fractions X_{DHAB} of the cationic lipid. The concentration was 1 mM in 5 mM Hepes, 0.1 mM EDTA, pH 7.4 and heating rate was 0.5 °C/min. The calibration bar represents 5 mJ^oC^{-1}.

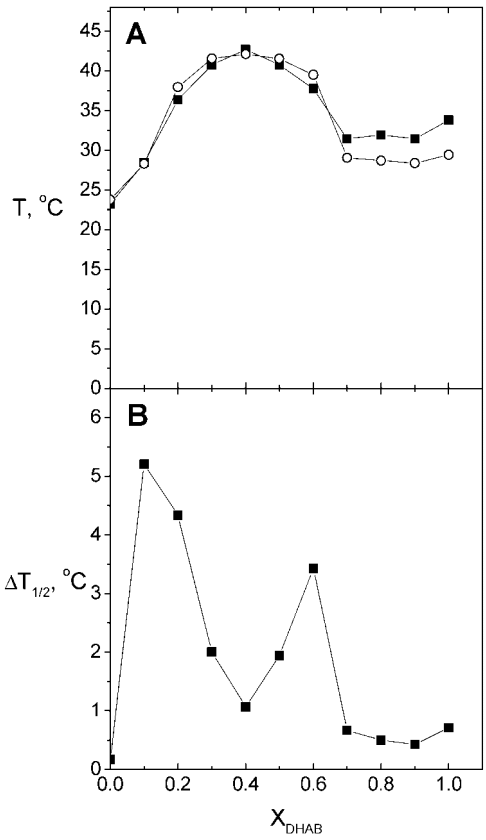

FIGURE 5.6 Panel A, Temperatures that exhibit the minima of first derivatives of DPH-PC fluorescence anisotropy vs. temperature scans of DHAB/DMPC/DPH-PC vesicles (■) and main transition temperatures (T_m) for DHAB/DMPC vesicles (○) plotted as a function of X_{DHAB}. **Panel B**, Widths of the main transition endotherms at the half height ($\Delta T_{½}$) for DHAB/DMPC vesicles plotted as a function of X_{DHAB}. Both T_m and $\Delta T_{½}$ values were obtained from DSC data shown in Figure 5.5.

resulting in a sigmoidal dependence of T_m on X_{DHAB}.

The cooperativity of transitions, evident as the width of the transition endotherms, changed as the surface charge density was varied (Fig. 5.5). To demonstrate this better the widths of the endotherms at the half height $\Delta T_{½}$ (McElhaney, 1982) were depicted as a function of X_{DHAB} (Fig. 5.6, panel B). These data revealed two maxima in $\Delta T_{½}$, at X_{DHAB} = 0.1 and 0.6 ($\Delta T_{½}$ = 5.21 and 3.42 ^{o}C, respectively), indicating low cooperativity of transition for these mixtures and a local minimum at X_{DHAB} = 0.4 with $\Delta T_{½}$ = 1.07 °C. At $X_{DHAB} \geq 0.7$ $\Delta T_{½}$ is low (between 0.43 and 0.71 °C) indicating higher cooperativity compared to other vesicle compositions investigated but still markedly lower than for neat DMPC vesicles ($\Delta T_{½}$ = 0.17 °C), which exhibited the highest cooperativity. However, it should be noted that for the samples demonstrating marked phase separation, i.e. at X_{DHAB} = 0.6, 0.7, and 0.8, the $\Delta T_{½}$ was measured at the half height of the highest endothermic peak and the wide shoulder at the higher temperatures was omitted (Fig. 5.5). The cooperativity of chain melting in these samples was thus overestimated.

5.2.2 Impact of surface electrostatics on DHAB/POPC monolayers

Compression isotherms of mixed DHAB/POPC monolayers were recorded while systemically varying X_{DHAB}. Analysis of mean molecular areas (Fig. 5.7) revealed that even a small fraction of DHAB (X_{DHAB} = 0.05) was able to condense POPC monolayer significantly and further increasing X_{DHAB} reduced mean molecular area until a minimum at $X_{DHAB} \approx 0.38$ (Fig. 5.7, panel A). After this minimum mean molecular area began to slowly rise up to X_{DHAB} = 1.0 but still remaining at lower values than measured for neat POPC monolayer. The condensing effect required PC headgroup and instead of condensation an expansion of monolayer presumably due to increasing Coulombic repulsion was evident when DHAB was mixed with neutral dioleylglycerol (III, Fig. 3). Addition of DNA into subphase had different impact on mean molecular area of the monolayer lipids depending on both X_{DHAB} and [DNA]. Accordingly, at [DNA] = 0.63 μM DNA caused pronounced condensation of mean molecular area at $X_{DHAB} < 0.5$ while at $X_{DHAB} > 0.5$ expansion of the monolayer due to DNA was evident (Fig. 5.7, panel B). However, at [DNA] = 1.88 μM condensation of the monolayer was observed irrespective of X_{DHAB} (Fig. 5.7, panel C).

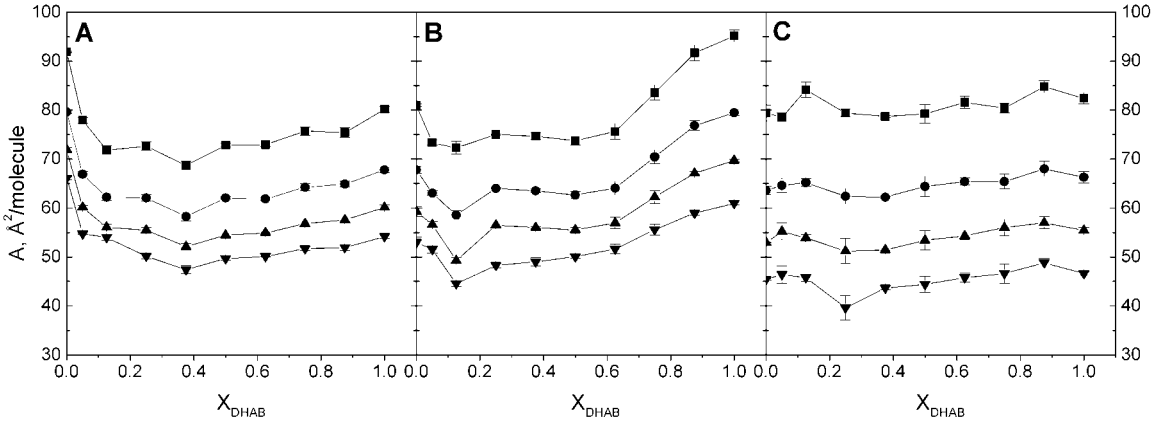

FIGURE 5.7 **Panel A**, Impact of X_{DHAB} on mean molecular area in compression isotherms of mixed DHAB/POPC films. The subphase was 5 mM Hepes, 0.1 mM EDTA, pH 7.4, and values of π were 10 (■), 20 (●), 30 (▲), and 40 (▼). Similar data were obtained also with, **Panel B**, 0.63 and, **Panel C**, 1.88 μM CT-DNA in the subphase.

5.2.3 Fluorescence spectroscopy

To obtain more detailed view on the molecular level phenomena induced by surface electrostatics and temperature in DHAB/DMPC liposomes emission spectra for DPH-PC as a function of X_{DHAB} were collected at selected temperatures (20, 35, and 48 °C) so as to cross phase boundaries revealed by DSC (Fig. 5.6, panel A).

X_{DHAB} had a drastic effect on the maximal emission intensity of DPH-PC I_{max} (Fig. 5.8, panel A). When mole fraction of DHAB was increased in DMPC vesicles I_{max} decreased slowly until at $0.3 \leq X_{DHAB} \leq 0.5$ significant quenching was observed with a local minimum centered at $X_{DHAB} = 0.4$. After this minimum I_{max} increased rapidly and reached a local maximum at $X_{DHAB} = 0.6$. At $X_{DHAB} > 0.6$ nearly linear decrease in I_{max} as a function of X_{DHAB} was evident that continued until $X_{DHAB} = 1.0$. It should be noted that the counterion of the cationic DHAB, bromide, is a collisional quencher and could thus contribute to the diminished fluorescence intensity. However, the concentration of Br^- is small in the fluorescence experiments (maximally 50 µM at $X_{DHAB} = 1.0$), which makes this possibility unlikely.

The wavelengths for the center of mass for the DPH emission peaks (λ_c) were calculated from the collected spectra and are depicted as a function of X_{DHAB} (Fig. 5.8, panel B). DPH fluorescence shifts to shorter wavelengths when the surrounding environment becomes more hydrophobic, e.g. when less water penetrates into hydrocarbon phase

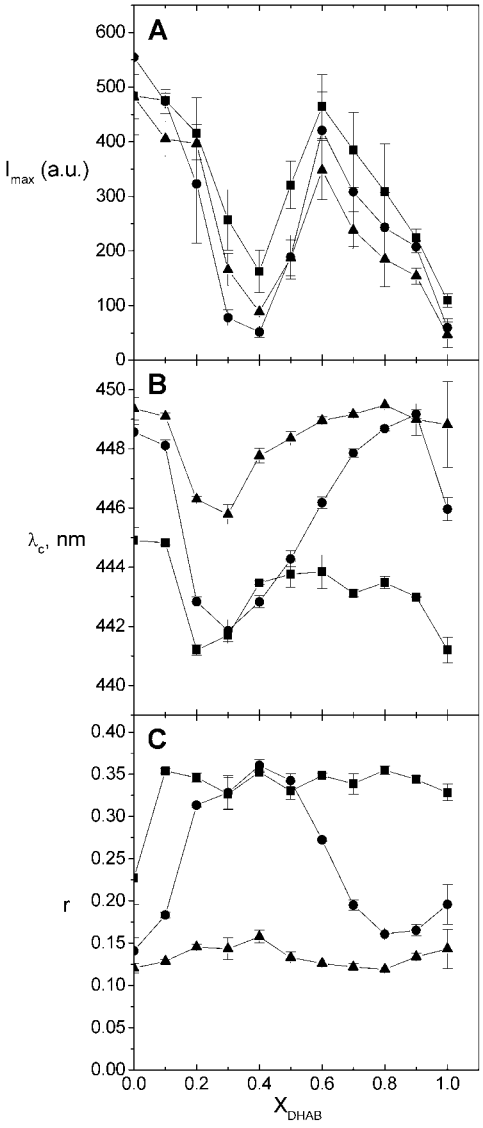

FIGURE 5.8 **Panel A**, Maximal emission intensity of DPH-PC (I_{max}), **Panel B**, spectral center of mass calculated from the emission spectra of DPH-PC (λ_c), and **Panel C**, emission anisotropy (r) recorded for DHAB/DMPC/DPH-PC vesicles depicted as a function of X_{DHAB}. Temperature was 20 (■), 35 (●), and 48 °C (▲). Total lipid concentration was 50 µM in 5 mM Hepes, 0.1 mM EDTA, pH 7.4. The error bars represent standard deviation calculated from at least three experiments.

of the lipid bilayer (Lakowicz, 1999). This is readily evident from our data. DPH in the fluid, disordered state vesicles at 48 °C exhibited λ_c in the range 446 – 450 nm, in contrast to vesicles in the gel state at 20 °C with $\lambda_c \approx 441 – 445$ nm. The same phenomenon was observed also for vesicles with $0.2 < X_{DHAB} < 0.6$ at 35 °C (i.e. in the gel state) having λ_c at approx. 441 to 446 nm.

The steady state anisotropy data for DPH are illustrated as a function of X_{DHAB} in Fig. 5.8, panel C. At 20 °C all vesicle compositions investigated in this study were in the gel state, in keeping with the high values for r. Similarly at 50 °C all vesicles were in fluid state with low values for r. Yet, at both of these temperatures local maxima in r at $X_{DHAB} = 0.4$ were observed, indicating tighter packing of the acyl chains. In keeping with phase behavior determined by DSC (Fig. 5.5) the DHAB/DMPC MLVs revealed composition dependent changes in r at 35 °C. More specifically at this temperature vesicles with $X_{DHAB} = 0.3$, 0.4, and 0.5 were in the gel state, whereas vesicles with $X_{DHAB} = 0.2$ and 0.6 were in the main transition regime, and all other compositions were in the fluid state, thus revealing pronounced changes in r as a function of X_{DHAB}. Importantly, as we did not determine the lifetime of the probe, these changes in r should in strict sense be taken as tentative only. However, in the light of the perfect alignment of the anisotropy data with all other measurements on the system at hand we may conclude r in this case to reflect changes in acyl chain order.

It is expected that I_{max} decreases with temperature and especially when T_m is exceeded because of enhanced collisions of the fluorophore with water upon increasing average intermolecular areas. However, I_{max} vs. temperature curve for vesicles with $X_{DHAB} = 0.4$ and 1.0 revealed different behavior of these two vesicle compositions demonstrating quenching of DPH emission (Fig. 5.9). For $X_{DHAB} = 0.4$ I_{max} first decreased as the temperature was elevated but suddenly increased at T = 42 °C, i.e. at T_m of these

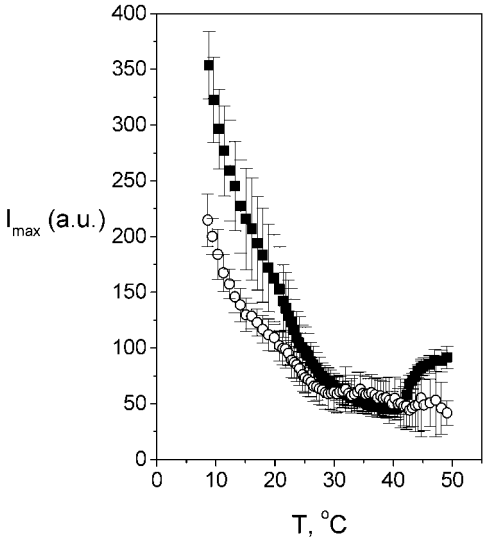

FIGURE 5.9 Maximal emission intensity of DPH-PC (I_{max}) DHAB/DMPC/DPH-PC vesicles shown as a function of temperature. X_{DHAB} was 0.4 (■) and 1.0 (○). Buffer was 5 mM Hepes, 0.1 mM EDTA, pH 7.4 and the total lipid concentration 50 μM. The error bars represent standard deviation calculated from at least three experiments.

vesicles. This is contrasted by vesicles with X_{DHAB} = 1.0 which exhibited steadily decreasing I_{max} as a function of temperature without discontinuities at T_m.

To evaluate the impact of surface electrostatics on above findings the same data were recorded for neat DHAB vesicles in the presence of varying [NaCl] (Fig. 5.10). Upon increasing [NaCl] from 0 to 50 mM I_{max} was drastically elevated at all temperatures, after which I_{max} decreased reaching a plateau at 75 ≤ [NaCl] ≤ 150 mM (Fig. 5.10, panel A). When [NaCl] was increased further to 200 mM I_{max} decreased significantly at T = 20 and 35 °C while at 48 °C it remained at approximately on the same level measured at [NaCl] = 150 mM. In these experiments macroscopic aggregation of the vesicles due to the added salt was observed. Accordingly, to evaluate the effect of salt in more detail static light scattering was measured (Fig. 5.10, panel B) and T_ms of the DHAB vesicles (Fig. 5.10, panel C) were determined from r vs. T scans similarly to the data presented earlier (see section 5.2.1 and Fig. 5.6, panel A). For vesicles below T_m, i.e. at 20 °C, markedly increased scattering due to salt was observed until [NaCl] = 150 mM after which intensity of scattered light significantly diminished at [NaCl] = 200 mM. As temperature exceeded T_m scattering diminished rapidly and for fluid state vesicles the intensity of scattered light was practically independent from [NaCl]. As [NaCl] was increased to 50 mM the value for T_m diminished to approx. 28.4 °C, subsequently reaching a minimum (approx. 27.5 °C) at [NaCl] = 150 mM. Upon further increase in [NaCl] the transition temperature again increased and at [NaCl] = 200 mM T_m was approx. 31 °C.

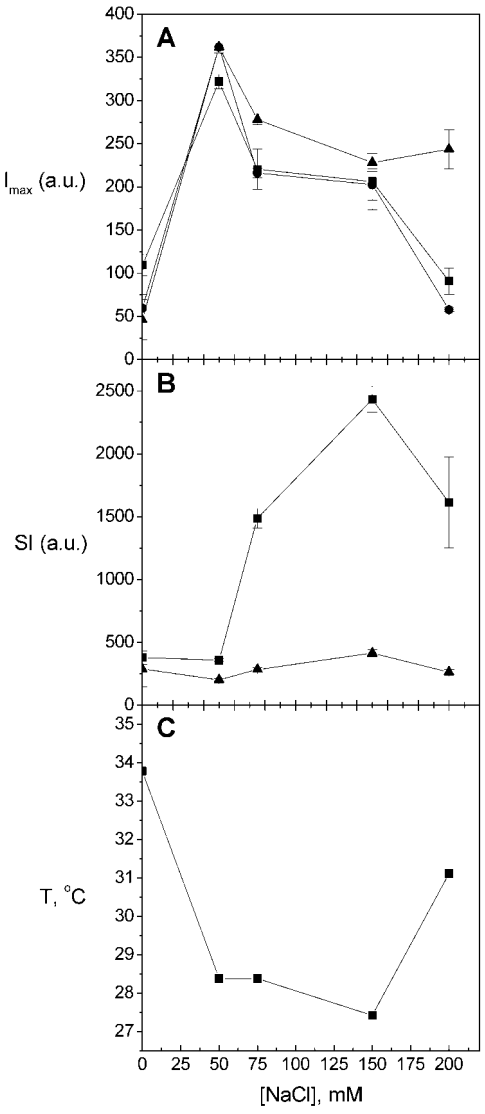

FIGURE 5.10 **Panel A**, Maximal emission intensity of DPH-PC (I_{max}), **Panel B**, integrated scattered intensity (SI), and **Panel C**, temperatures that exhibit the minima of first derivatives of DPH-PC fluorescence anisotropy vs. temperature scans recorded for DHAB/DPH-PC vesicles depicted as a function of [NaCl]. In the panels A and B temperatures were 20 (■), 35 (●), and 48 °C (▲). Total lipid concentration was 50 μM in 5 mM Hepes, 0.1 mM EDTA, pH 7.4 with indicated [NaCl]. The error bars represent standard deviation calculated from at least three experiments.

5.2.4 Fourier transform infrared spectroscopy

To obtain more detailed view on the phase behavior of DHAB/DMPC vesicles FTIR spectra were recorded for six different vesicle compositions, viz. X_{DHAB} = 0.0, 0.2, 0.4, 0.6, 0.8, and 1.0. Shift in the wavenumbers of the -CH_2- symmetric stretching mode ($\upsilon_s CH_2$) at ~2,850 cm^{-1} was employed to monitor the *trans→gauche* isomerization of the lipid acyl chains and to detect the main phase transition (Lewis and McElhaney, 1996). The FTIR data on -CH_2- vibrational modes were consistent with the phase behavior of DHAB/DMPC vesicles determined by DSC and fluorescence spectroscopy (Figs. 5.6, panel A). Accordingly, as temperature was elevated from 20 to 48 °C a shift in the wavenumber of $\upsilon_s CH_2$ absorption from ≤ 2,851 cm^{-1} to ≥ 2,853 cm^{-1} was observed for all vesicle compositions indicating transition from gel to fluid phase (Fig. 5.11, panel A). At 35 °C a significant shift to lower wavenumbers was evident for the vesicles with X_{DHAB} = 0.2 and 0.4 in keeping with DSC and fluorescence data indicating these vesicles to be in the gel state, while other compositions are in the fluid state or in the main transition regime (X_{DHAB} = 0.6). However, also at X_{DHAB} = 1.0 a shift to lower wavenumbers not expected based on the fluorescence and DSC measurements was observed. At X_{DHAB} = 0.6 and at 35 and 48 °C a marked shift to higher wavenumbers was recorded that was absent in the data recorded for gel state vesicles at 20 °C.

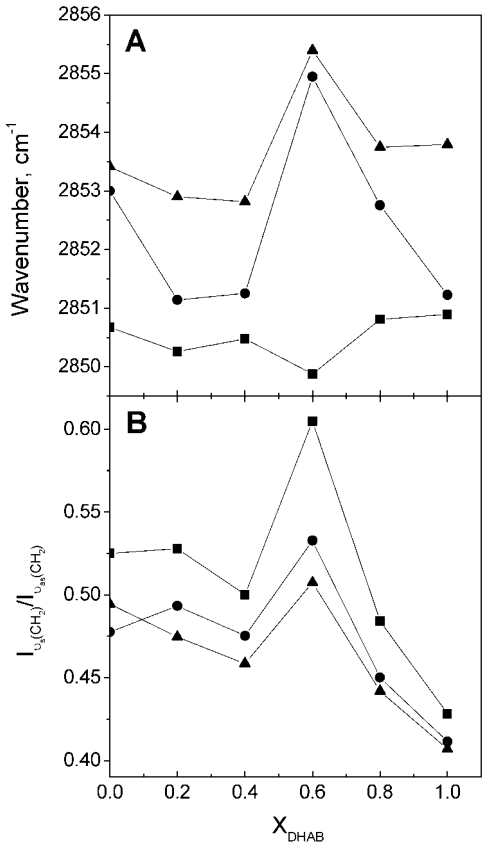

FIGURE 5.11 **Panel A**, The wavenumber shift in -CH_2- symmetric stretch IR absorption band as a function of X_{DHAB}. **Panel B**, The ratio of integrated peak intensities of symmetric and antisymmetric -CH_2- stretching modes in DHAB/DMPC vesicles as a function of X_{DHAB}. Temperature was 20 (■), 35 (●), and 48 °C (▲). Total lipid concentration was 10 mg/ml in Millipore water.

O'Leary and Levin (1984) have reported that interdigitation of DMPC bilayer can be observed by Raman spectroscopy as a decrease of

the intensity ratio of the symmetric and antisymmetric methylene stretching modes ($I(\upsilon_s CH_2)$ / $I(\upsilon_{as} CH_2)$). These authors suggested that the decrement is due to broadening and a concomitant decrease in $I(\upsilon_s CH_2)$ because of augmented chain-chain interactions in the interdigitated phase. We calculated this ratio from our FTIR data and an almost linear decrease in $I(\upsilon_s CH_2)$ / $I(\upsilon_{as} CH_2)$ ratio at all temperatures when $X_{DHAB} > 0.6$ was evident (Fig. 5.11, panel B).

5.3 SPONTAENOUS SELF-ASSEMBLY OF CATIONIC GEMINI SURFACTANT INTO GIANT VESICLES (IV)

Aqueous solutions of the dicationic gemini surfactant M-1 (for structure see Fig. 4.1) demonstrated peculiar behavior as observed by visual inspection when NaCl concentration and temperature were varied. In brief, when dispersed in water as well as in [NaCl] < 1.5 M solutions of 1 mM M-1 were optically clear suggesting surfactant to be organized into micelles or small vesicles, while at [NaCl] = 1.5 and 2 M and at approx. 60 ^{o}C solutions were opalescent and bluish. At [NaCl] = 3 M the surfactant solutions became cloudy even at ambient temperature (approx. 21 ^{o}C). Cooling M-1 in [NaCl] = 1.5 and 2 M back to ambient temperature resulted in optically clear solutions indicating that process is readily reversible. Incubation for approx. 12 h at ambient temperature revealed floating macroscopic aggregates that were easily disrupted by either vigorous mixing or heating.

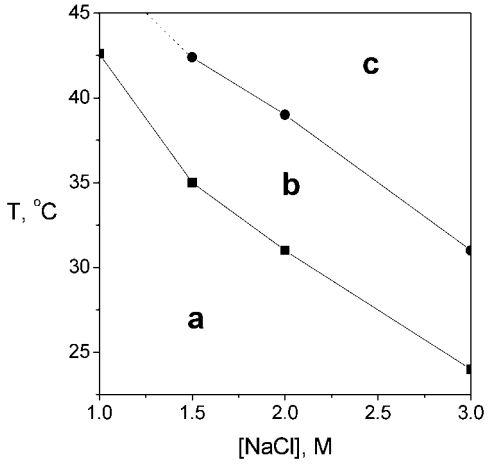

FIGURE 5.12 Tentative [NaCl] vs. temperature vesicle shape/size phase diagram derived from microscopy experiments of 1 mM M-1 dispersion. **a,** Submicroscopic structures, **b,** large GVs, tubular, and cytomimetic structures in the vicinity of the air/water interface, and **c,** small GVs throughout water phase.

Optical microscopy of M-1 dispersions with varying [NaCl] revealed formation of giant vesicles (GVs) as temperature was elevated. To better demonstrate this phenomenon a tentative structural phase diagram was constructed that illustrates the transition temperatures T_g and T_s, defined as the temperatures at which large GVs (T_g) and smaller GVs (T_s) emerge, as a function of [NaCl] (Fig. 5.12). At [NaCl] = 0.5 M no visible structures were observed within the examined temperature range (from 24 to 50 ^{o}C) and at [NaCl] = 1 M only occasional GVs were seen at T > 43 ^{o}C. In contrast, at [NaCl] > 1 M a sequence of transitions became evident, exemplified by micrographs taken at [NaCl] = 2 M upon heating (Fig. 5.13). More specifically, no visible structures were observed at 24 ^{o}C while at approx. 29 ^{o}C very long tubular structures appeared near the air/water interface of the solution (Fig. 5.13, panel a). With further increase in temperature to $T_g \approx 33$ ^{o}C these structures fused within seconds to GVs that were present also beneath the surface of the solution (Fig. 5.13, panel b). The average diameter of GVs varied between approx. 30 - 50 μm

while also larger vesicles were occasionally seen. In this temperature regime GVs exhibited heterogeneous morphologies with some resembling living cells with internal organelles (Fig. 5.13, panel b, insets). At T > 36 °C the size of the GVs started to decline and upon exceeding T_s at approx. 40 °C morphologically homogenous smaller GVs (diameters of ~10-15 μm) were evident throughout the sample cell (Fig. 5.13, panel c). No further changes were seen upon heating to 50 °C suggesting the bluish appearance of M-1 solution at 60 °C to be caused by light scattering due to numerous population of smaller GVs. The above sequence of shape/size transitions was reversed upon cooling back to 24 °C. Interestingly, the air/water interface (with the surfactant monolayer) seems to be essential for the formation of the more complex aggregates i.e. tubular and cytomimetic vesicle morphologies as they were absent when experiments were conducted in a small concealed glass compartment instead of an open chamber. However, transition to larger GVs (at ~31 °C) and also to numerous smaller GVs (at ~39 °C) was observed also under these conditions. This transition was quantified by measuring diameters of aggregates formed by dynamic light scattering. In brief, during a temperature scan of 1 mM M-1 in 2 M NaCl a sharp transition from small vesicles with diameters of approx. 40 nm into GVs with diameters of approx. 11 μm was evident at $T_s \approx 40$ °C (IV, Fig. 4). The preceding transition into larger, more heterogeneous GVs could not be evaluated by dynamic light scattering because this transition takes place exclusively at the air/water interface.

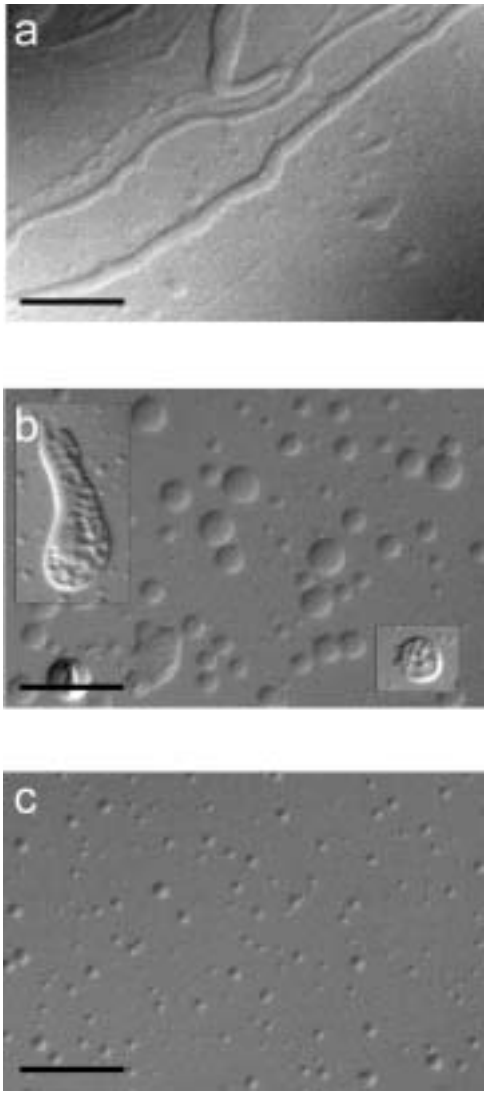

FIGURE 5.13 Microscopy images of 1 mM M-1 solution with 2 M NaCl at approx. **a,** 30 **b,** 33, and **c,** 43 °C**.** The scale bars represent 100 μm.

The above phenomenon was further characterized by monolayer and DSC experiments. Accordingly, the lift-off areas ($A_{lift\text{-}off}$) were determined from compression isotherms of M-1 monolayers as a function of [NaCl] (Fig. 5.14, panel A) and revealed progressive decrease from approx. 150 $Å^2$/acyl chain at 150 mM NaCl to a minimum at [NaCl] = 2 M. Further increasing [NaCl] to 3 M resulted in expansion of $A_{lift\text{-}off}$. During DSC heating scan at [NaCl] = 150 mM 1 mM M-1 dispersion exhibited a single endotherm with T_m at 14.7 ^oC. In keeping with diminished $A_{lift\text{-}off}$ increasing [NaCl] elevated T_m nearly linearly reaching 21.4 ^oC at 3 M salt (Fig. 5.14, panel B). The enthalpies contained in transition endotherms (ΔH) were also calculated. As [NaCl] was increased to 0.5 M ΔH demonstrated a rapid increment where after a plateau until [NaCl] = 1 M was evident (Fig. 5.14, panel C). However, at [NaCl] > 1 M ΔH abruptly decreased to the approximately same level as observed at [NaCl] = 150 mM.

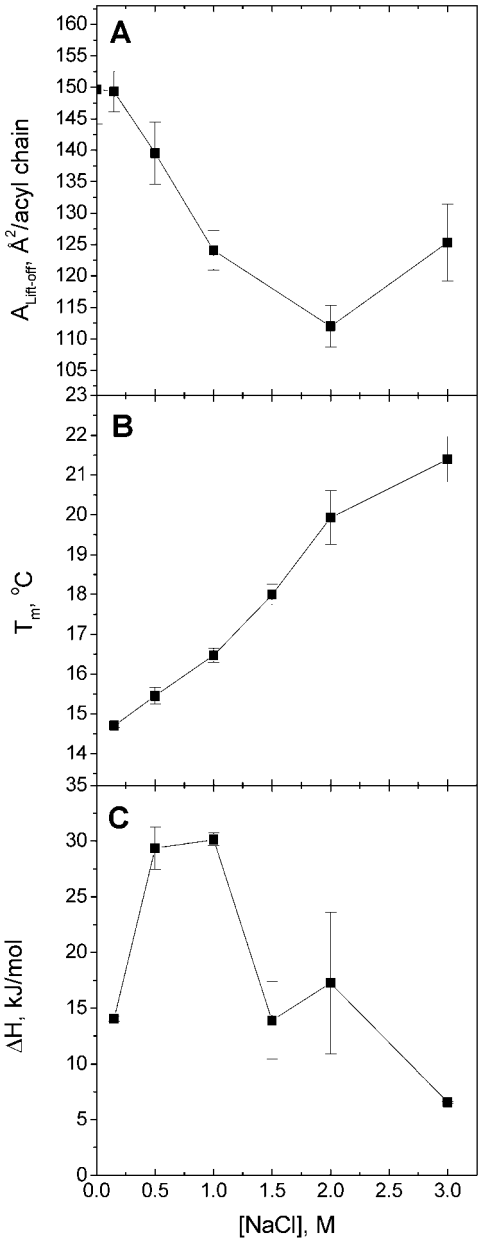

FIGURE 5.14 **Panel A,** Lift-off areas ($A_{Lift\text{-}off}$) from monolayer compression isotherms recorded as a function of [NaCl] in the subphase. **Panel B,** Main transition temperatures (T_m) obtained for 1 mM M-1 dispersions from DSC measurements as a function of [NaCl]. **Panel C,** Enthalpies contained in the transition endotherms (ΔH) obtained from DSC measurements as a function of [NaCl]. Error bars represent standard deviation calculated from at least three measurements.

6. DISCUSSION

Theme unifying the four original contributions included in this thesis is cationic lipids and their properties as a supramolecular assembly. Publication I considers mainly the impact of the surface charge density on the organization of mixed DHAB/DMPC vesicles and how this is reflected in mode of interaction of these liposomes with DNA and transfection efficiency. Publication II presents a more detailed investigation on the molecular level changes in DHAB/DMPC vesicles when X_{DHAB} is varied and provides evidence for interdigitation due to Coulombic repulsion in high surface density regime. The monolayer experiments of publication III complete the characterization of mixed DHAB/phosphocholine model membranes and strengthen the conclusions made based on publications I and II. The last publication (IV) describes spontaneous formation of giant vesicles by a cationic gemini surfactant that is dependent on NaCl concentration and temperature. Previously published mechanisms for mesoscale transitions fail to explain this phenomenon and, accordingly, a novel mechanism that controls the membrane curvature at mesoscopic scales is proposed.

It is must be noted that instead of pure DHAB a stoichiometric mixture of DHAB and N,N-dimethyl-3,4-dimethylpyrrolidium bromide was used in experiments described in publications I and III. The reason for this as well as appropriate corrections to articles I and III are described in detail in correction article that can be found in Original publications section after reprints of original contributions. Importantly, the water-soluble pyrrole did not affect monolayer compression isotherms of DHAB or phase behavior of binary DHAB/DMPC vesicles as determined by DSC. Accordingly, the data as well as conclusions presented in publications I and III remain valid. Corrected CL/DNA ratios and lipid nomenclature are used throughout the thesis.

6.1 SURFACE CHARGE DENSITY DETERMINES THE TRANSFECTION EFFICIENCY OF DHAB/DMPC VESICLES

Lipofection efficiency of DHAB/DMPC vesicles is critically dependent on surface charge density. While liposomes with $X_{DHAB} \geq 0.50$ showed transfection efficiencies comparable to commercial lipofection reagents, for vesicles with $X_{DHAB} = 0.25$ only negligible transgene expression was observed (Fig. 5.1). The total amount of cationic DHAB and plasmid was kept constant in transfection experiments thus excluding these variables as a cause for observed dependence (see section 4.2.1 for details of liposome preparation). Importantly, also cytotoxicity of DHAB/DMPC lipoplexes remained essentially constant when X_{DHAB} was varied (Fig. 5.2). Importance of surface charge density on transfection efficiency of lipoplexes has been later confirmed by Lin and co-workers (Lin et al., 2003). These authors further demonstrated that dependence on surface charge density concerns lamellar lipoplexes but not lipoplexes preferring H_{II} phase (see Fig. 2.5), and that transfection efficiency abruptly increases upon exceeding critical surface charge density regardless of the valence of the cationic lipid employed. This together with our results suggests that surface charge density represents a universal determinant for efficiency of lipofection by lamellar lipid-DNA complexes.

A possible explanation for increased transfection is enhanced ability of DHAB/DMPC liposomes with $X_{DHAB} > 0.50$ to condense DNA suggested by augmented light scattering (Fig. 5.3) and further confirmed by ethidium bromide intercalation assay (Fig. 5.4). It is well known that condensation of DNA protects plasmid from degradation before internalization by the cells (Xu and Szoka, 1996; Bhattacharya and Mandal, 1998) and enables formation of compact and more dense lipoplexes that could promote e.g. nuclear delivery of the plasmid. However, DNA condensation required slightly higher surface charge density than was needed to achieve efficient transfection, viz. $X_{DHAB} > 0.50$ and $X_{DHAB} \geq 0.50$, respectively. A plausible explanation for this is provided by differing lengths of the DNA molecules used. DNA condensation after binding to cationic liposomes is a coil-to-globule transition that is driven by charge neutralization of anionic phosphate moieties as well as counterion release counteracting decrease in conformational entropy accompanying the collapse of DNA molecule (Bloomfield, 1991; 1996; 1998; Gelbart et al., 2000). Accordingly, condensation of longer calf thymus DNA employed in light scattering and EtBr intercalation experiments causes larger decrement in conformational entropy and thus requires higher

surface charge density to ensue than shorter circular plasmid DNA (length approx. 4.7 kb) used in transfection studies.

6.2 IMPACT OF SURFACE CHARGE DENSITY ON DHAB/DMPC MEMBRANES

6.2.1 Reorientation of phosphocholine headgroup

Mixed DHAB/DMPC membranes revealed thermal phase behavior, which is at first glance counterintuitive. Accordingly, T_m followed sigmoidal dependence on X_{DHAB} with a maximum at $X_{DHAB} = 0.40$ and a local minimum at $X_{DHAB} \approx 0.90$ while instead decreased T_m was expected for mixed bilayers when compared to single component systems (Fig. 5.6, panel A). However, this behavior is readily explained by electrostatic interactions between positively charged quaternary ammonium moiety of DHAB headgroup and zwitterionic headgroup of phosphocholine. More specifically, cationic headgroup of DHAB binds to anionic phosphate of P^--N^+ dipole inducing reorientation of the dipole from horizontal to more vertical position with respect to bilayer plane by virtue of Coulombic repulsion between the two positive charges (Fig 6.1). Reorientation of P^--N^+ dipole together with reduced hydration of headgroups due to charge neutralization of phosphate (Zuidam and Barenholz, 1997; Hirsch-Lerner and Barenholz, 1999) decrease the area occupied by PC headgroup thus causing apparent condensation of POPC monolayer when even small fraction of DHAB is introduced into membrane (Fig. 5.7, panel A). The condensation upon addition of cationic lipids has been demonstrated also for sphingosine/POPC (Säily et al., 2003) and DMTAP/DMPC monolayers (Zantl et al., 1999). For lipid bilayers electrostatic headgroup reorientation has been shown in pioneering NMR studies by Seelig and co-workers (Seelig et al., 1987; Scherer and Seelig, 1989) and further confirmed by DSC (Zantl et al., 1999; Silvius, 1991) as well as molecular dynamics simulations (Bandyopadhyay et al., 1999; Gurtovenko et al., 2004). To summarize, diminished average area of lipid molecules due to electrostatic reorientation of P^--N^+ dipole in mixed DHAB/DMPC bilayer allows for augmented chain-chain interactions and thus increases thermal energy required for *trans→gauche* isomerization of acyl chains and elevates T_m (Figs. 5.5 and 5.6).

6.2.2 Interdigitation induced by surface charge density

After a maximum at X_{DHAB} = 0.40 T_m decreased progressively until plateau was reached at X_{DHAB} > 0.60 (Fig. 5.6, panel A). This decrement is consistent with Gouy-Chapman theory of charged interfaces as increasing concentration of DHAB augments Coulombic repulsion between cationic lipids thus expanding the membrane and reducing chain-chain interactions (Cevc, 1990). However, the plateau at X_{DHAB} > 0.60 and eventual increment in T_m at X_{DHAB} > 0.90 observed also in DSC study by Silvius (1991) are in contrast with the classical theory. Moreover, expansion of molecular areas in DHAB/POPC monolayers (Fig. 5.7) and molecular dynamic simulations on DMTAP/DMPC bilayers (Gurtovenko et al., 2004) at high surface charge densities contradict the observed thermal phase behavior of DHAB/DMPC vesicles. Accordingly, it seems evident that in high surface charge density regime DHAB/phosphocholine bilayers undergo reorganization that cannot take place either in lipid monolayers restricted to two dimensions or in molecular dynamics simulations on lipid bilayers with simplified molecular interactions and limited timescale.

Upon exceeding X_{DHAB} = 0.50 the amount of unpaired DHAB molecules increases and a population of cationic lipids with well hydrated headgroups and mutual Coulombic repulsion at headgroup level emerges. This results in change in the effective shape of DHAB molecules as their average headgroup area is increased while area occupied by the acyl chains remains essentially

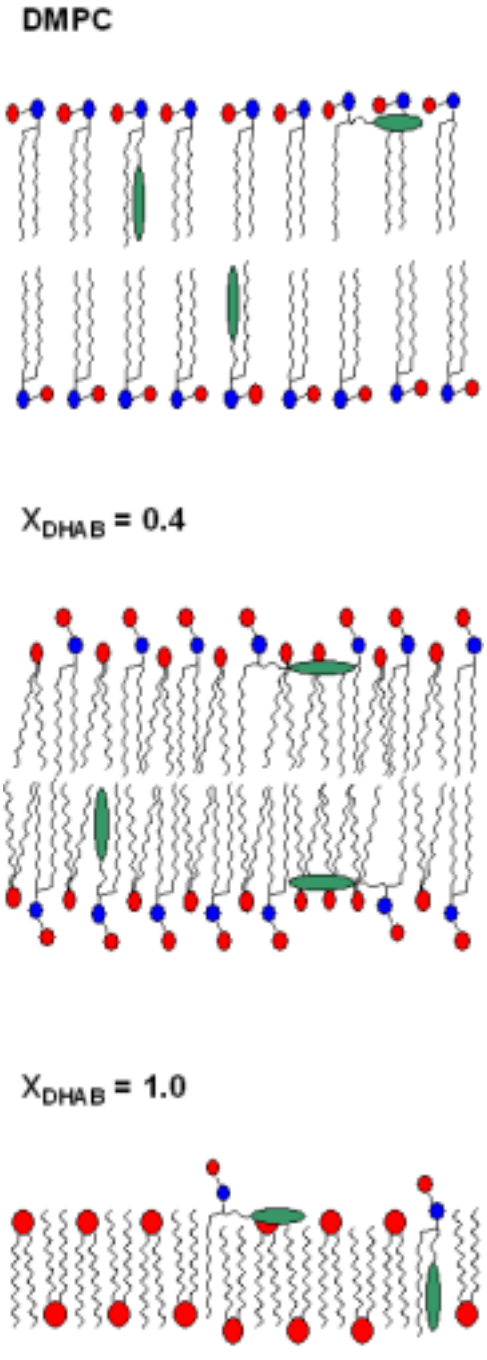

FIGURE 6.1 Schematic illustration of the DHAB/DMPC/DPH-PC bilayer at X_{DHAB} = 0, 0.4, and 1.0 representing the suggested impact of increasing surface charge density on the molecular organization of the membrane. Red circles represent positive and blue negative charges in the headgroups. The DPH moiety of the DPH-PC is depicted by green oval.

constant (see section 2.1.1). Large headgroup area favors lipid packing into conventional micelles (Israelachvili, 1991) or alternatively to chain interdigitated bilayer phase (Pascher et al., 1992). Haas et al. (1999) have reported X-ray diffraction data indicating reduced membrane thickness for DHAB bilayers that would be compatible with interdigitated chains. Similarly, X-ray study by Pohle et al. (2000) suggested interdigitated bilayers in DMTAP/DMPC vesicles at high surface charge density. Accordingly, formation of an interdigitated phase would provide a feasible explanation for discontinuity in the phase diagram of mixed DHAB/DMPC vesicles as it allows to maximize the distance between headgroups while simultaneously resulting in tight packing of acyl chains in the hydrocarbon region of bilayer (Fig 6.1) evident as elevated T_m and diminished $\Delta T_{½}$ (Fig. 5.6). Furthermore, the discrepancy between DSC data and results from monolayers as well as computer simulations is also explained as interdigitation is impossible in lipid monolayers and easily missed in a molecular dynamics study.

Fluorescence spectroscopy was used to evaluate the possibility of interdigitation more thoroughly. In DPH-PC the fluorescent DPH moiety is attached to *sn*-2 chain of a phospholipid analog (Fig. 4.1) and fluctuates between two conformations with one population aligned with the acyl chains and other residing parallel to membrane interface (Pebay-Peyroula et al., 1994; Alakoskela and Kinnunen, 2004). Quantum yield of the latter population is reduced due to polar environment at the interface, while in an interdigitated bilayer also the population normally buried deeply in the hydrophobic core of the bilayer becomes exposed to polar lipid headgroups and water molecules (Fig. 6.1) resulting in prominent quenching of DPH emission (Nambi et al., 1988; Hutterer et al., 1997). Accordingly, significant quenching of DPH-PC fluorescence emission at $X_{DHAB} > 0.60$ (Fig. 5.8, panel A) is in keeping with transition to interdigitated phase. Moreover, interdigitation is suggested also by FTIR data (Fig. 5.11, panel B) demonstrating a decrement in $I(\upsilon_s CH_2)$ / $I(\upsilon_{as} CH_2)$ ratio shown to correlate with interdigitation in DMPC bilayers (O'Leary and Levin, 1984). However, I_{max} of DPH fluorescence demonstrates also a local minimum at $X_{DHAB} = 0.40$ (Fig. 5.8, panel A) that cannot be explained by interdigitation induced by elevated surface charge density. Plausible explanation for this minimum is provided by tight packing of membrane hydrocarbon phase at $X_{DHAB} = 0.40$ indicated by high r (Fig. 5.8, panel C), a maximum in T_m, and a local minimum in $\Delta T_{½}$ (Fig. 5.6). Relatively bulky DPH moiety of DPH-PC does not fit easily into crowded acyl chain region of the tightly packed bilayer and the conformation in which DPH moiety lays planar in the membrane interface is favored with subsequent fluorescence quenching (Fig. 6.1). Consistent with this interpretation I_{max}

increases significantly for vesicles with X_{DHAB} from 0.30 to 0.50 upon exceeding T_m, i.e. when more loose acyl chain packing allows DPH to accommodate into hydrocarbon phase more easily (Fig. 5.9). In contrast, I_{max} is insensitive to T_m for vesicle compositions suggested to be in interdigitated phase (Fig. 5.9).

Interestingly, DPH-PC fluorescence decreases nearly linearly at $X_{DHAB} > 0.60$ until a minimum at $X_{DHAB} = 1.0$ (Fig. 5.8, panel A) suggesting interdigitation to proceed gradually as a first order process rather than as an abrupt phase transition at $X_{DHAB} = 0.60$. In keeping with the above phase separation is evident in DSC traces recorded for vesicles with $0.60 \leq X_{DHAB} \leq 0.80$ (Fig. 5.5). Accordingly, it is likely that interdigitated domains appear in the DHAB/DMPC bilayers at $X_{DHAB} > 0.50$ and their size progressively increases as fraction of DHAB in the system is elevated until a percolation threshold at $X_{DHAB} \approx 0.90$ after which entire bilayer is interdigitated.

If electrostatic repulsion between cationic headgroups is the driving force for interdigitation screening these charges by adding NaCl into buffer should abolish the interdigitation. I_{max} did indeed increase when NaCl was present suggesting loss of interdigitation (Fig 5.10, panel A). However, at [NaCl] > 150 mM and at 20 and 35 ^oC I_{max} again decreased. This behavior is explained by aggregation of DHAB vesicles in the high salt concentration evident from the light scattering data (Fig. 5.10, panel B). Accordingly, as the electrostatic screening decreases Coulombic repulsion between the cationic charges of DHAB within the bilayer and reverts normal bilayer packing, repulsion between the vesicles is simultaneously diminished resulting in vesicle aggregation. At relatively low [NaCl] aggregation was observed as an augmented light scattering for gel state vesicles whereas at [NaCl] > 150 mM the macroscopic aggregates were evident, with precipitation apparent as diminished I_{max} and scattered intensity. For fluid state vesicles scattering values were low throughout the [NaCl] range studied indicating absence of aggregation. In keeping with this the I_{max} measured at [NaCl] > 150 mM for fluid DHAB vesicles (at 48 ^oC) is of the same magnitude as the values measured at lower [NaCl]. The loss of interdigitation is evident also from T_ms determined from DPH-PC r vs. T scans (Figure 5.10, panel C). More specifically, T_m decreases at [NaCl] from 50 to 150 mM in keeping with diminished chain-chain interactions. At [NaCl] = 200 mM T_m again increases due to efficient electrostatic screening that reduces effective headgroup area of DHAB and causes augmented acyl chain packing.

To conclude, transition from normal bilayer packing of lipids into interdigitated bilayer due to Coulombic repulsion between cationic lipids is suggested. Formation of interdigitated phase has been previously shown for cationic P-O-ethyl phosphocholines (Lewis et al., 2001; Winter et al., 2001; Koynova and MacDonald, 2003; 2004). However,

very large headgroup of these lipids favors interdigitation even in the absence of electrostatic repulsion while small headgroup of DHAB is unlikely to induce interdigitation by steric mechanism. Intriguingly, this implies that interdigitation could be a general property of lipid membranes with sufficiently high molar fraction of charged lipids. Moreover, DHAB vesicles seem to be interdigitated even in the fluid state as I_{max} of DPH-PC is not affected upon exceeding T_m (Fig. 5.9)

6.2.3 Interdigitation and transfection

Interdigitation at $X_{DHAB} > 0.50$ seems at first glance to be irrelevant to transfection efficiency as it is abolished both by physiological ionic strength (Fig. 5.10, panel A) and complexation with DNA (unpublished data). However, the compelling association between interdigitation and increased lipofection efficiency at $X_{DHAB} > 0.50$ deserves further discussion. To this end Lin et al. (2003) demonstrated by Laser scanning confocal microscopy that it is *the endosomal escape* of plasmid DNA (see also section 2.3.3) that is enhanced upon exceeding the surface charges density threshold required for efficient lipofection. Moreover, another study indicated that a surfactant exhibiting vesicle→micelle transition in the endosomal pH promotes release of DNA from the endosomes although lipid-DNA complexes itself adapt lamellar bilayer structure (Fielden et al., 2001). Accordingly, it seems feasible that also lipids with latent tendency to form assemblies with positive curvature such as conventional micelles and interdigitated bilayers are capable of disrupting endosomal membranes and promoting efficient lipofection. Furthermore, interdigitation of mixed cationic lipid/phosphocholine bilayers provides a novel mechanism for cytotoxic effects of lipoplexes since it is known that cationic lipids readily mix with lipids of cellular membranes (Hui et al., 1996).

6.3 MEMBRANE CURVATURE SLAVED BY A COMMENSURATE COUNTERION LATTICE

Micrographs taken from 1 mM M-1 solution (Fig. 5.13) illustrate a dramatic mesoscale transition whereupon large tubular structures and giant vesicles (GVs) instantaneously appear at specific temperatures compiled in a tentative structural phase diagram (Fig. 5.12). Dynamic light scattering experiments have indicated M-1 to form spherical and rod-like micelles in low ionic strength medium, with hydrodynamic radii of 6 and 35 nm, respectively (Mancini et al., unpublished data). Hence it is evident that a significant increment in packing parameter *p* (see section 2.1.1) is required for M-1 to adapt into bilayers of GVs instead of micelles. Analogously to previously described loss of interdigitation in DHAB vesicles upon addition of NaCl (section 6.2.2), electrostatic screening of dicationic headgroups of M-1 by relatively high NaCl concentration reduces the effective area occupied by the headgroup providing mechanism for increase in *p*. In keeping with the above compression isotherms of M-1 recorded with varying [NaCl] in the subphase revealed a marked decrease in $A_{lift\text{-}off}$ when [NaCl] was elevated (Fig. 5.14, panel A) and DSC data demonstrated an increasing trend in T_m as function of [NaCl] in accord with augmented acyl chain packing in the hydrocarbon phase (Fig. 5.14, panel B). While increment in *p* is certainly a prerequisite for GV formation it is not an adequate explanation *per se* for the observed phenomenon. Accordingly, in large supramolecular assemblies such as liposomes consisting of numerous lipid molecules (from hundreds of thousands molecules in LUVs to billions in GVs) the estimated change in *p* of an individual molecule would be minute between submicroscopic liposomes and GVs. In addition, the critical importance of temperature is difficult to explain in terms of effective shape.

It seems obvious that a novel mechanism controlling the membrane curvature has to be involved with phenomenon at hand. To this end we propose that the dicationic headgroup of M-1 with fixed distance between charges (Fig. 4.1) could act as a nucleation center for Cl^- counterions to form a commensurate pseudocrystalline ion lattice on the membrane surface. This ion-counterion lattice would form only above threshold [NaCl] and is expected to be sensitive to temperature as well as phase state of the nucleating membrane. Accordingly, in order to adapt mean molecular areas to spacing preferred by ion lattice lipids have to be rather mobile, i.e. membrane has to be in fluid state. Yet, very elastic membrane, as e.g. in the gel-fluid co-existence regime (Evans and Kwok, 1982), would not form stable enough platform for lattice to form. In keeping with the above GV formation is observed at $T >> T_m$. The NaCl

crystal on the surface of lipid membrane favors planar geometry slaving membrane curvature and thus enforces formation of GVs instead of submicroscopic lipid aggregates with higher positive curvature. Formation of pseudocrystalline lattice on membrane provides also explanation for observed decrement in ΔH at [NaCl] > 1 M that otherwise seems to be in contrast with concomitant increment in T_m (Fig. 5.14, panel C). More specifically, regular spacing of the counterion lattice organizes cationic lipids into regular array preventing augmented acyl chain packing thus reducing enthalpy of transition. Providing direct evidence for presence of such a counterion lattice is difficult or even impossible by present means. However, indirect evidence presented here as well as observation that isomers of M-1 differing from M-1 only in stereochemical conformation of the spacer and thus having slightly different spacing between cationic charges of the headgroup interact vigorously with NaCl solution forming crystalline aggregates (unpublished observation). Accordingly, a special interaction between these gemini surfactants and Cl^- counterions seems plausible.

A surfactant capable of spontaneous formation of GVs that can be regulated by [NaCl] and temperature opens road for applications requiring precisely controlled self-assembly such as lipoplex design and liposomal drug delivery. Importantly, this observation clearly demonstrates that complex morphological transitions of cell sized lipid assemblies are possible in the absence of proteins. To this end liposomes have been proposed to be an important intermediate in origin of life and so-called protocell is suggested to consist of only lipid membranes and self-replicating RNA (Luisi et al., 1999; Szostak et al., 2001). Mechanisms of dramatic reorganizations of cellular membranes such as vesiculation and subsequent reappearance of nuclear membrane during mitosis (Gant and Wilson, 1997) as well as morphological changes of mitochondrial membranes in response to changes in metabolical state of the cell (Griparic and van der Bliek, 2001) remain elusive. Intriguingly, charged lipids are present in membranes of both above organelles, viz. cationic sphingosine is found in nuclear membranes and natural anionic gemini amphiphile cardiolipin, known to form complex mesoscale aggregates in presence of $CaCl_2$ (Lin et al., 1982), in mitochondrial membranes. Accordingly, formation of pseudocrystalline counterion lattices acting in concert with protein machinery could provide an important mechanism for morphological transitions of cellular organelles that could be readily regulated by counterion concentration, for instance.

ACKNOWLEDGEMENTS

This work was carried out at the Institute of Biomedicine/Biochemistry (formerly known as Department of Medical Chemistry) during the years 1999-2005. I thank professors *Olli Jänne*, *Ismo Virtanen*, and *Esa Korpi* for putting facilities at my disposal.

My deepest gratitude goes to my supervisor professor *Paavo Kinnunen*. Paavo is an endlessly innovative scientist whose passionate and imaginative attitude towards biophysics has made great impact on me. Moreover, under Paavo's leadership Helsinki Biophysics and Biomembrane Group has become internationally renowned research group with top-of-the-line instrumentation and relaxed working atmosphere. Six years in HBBG can change a medical student into a scientist.

It has been a great pleasure to work in the same project with *Matti Säily*, MD. In addition to close scientific collaboration we have shared numerous less scientific but as important moments during the medical school, traveling abroad, as well as in countless social occasions. *Juha-Matti Alakoskela*, MD is an irreplaceable source of biophysical knowledge. His collaboration and several long discussions with him have made this thesis a lot better and accurate. Matti and Juha-Matti are also thanked for their valuable comments on manuscript of this thesis. *Mikko Parry*, MD deserves special mention because of his expert advice with computers and other technical gadgets. I am also indebted to other co-authors with whom I have written the original contributions of this thesis: *Juha Holopainen*, MD PhD, *Tommi Paukku*, MD PhD, *Paola Luciani*, MSc, *Stefano Borocci*, PhD, and professor *Giovanna Mancini.* I wish to thank past and present members of HBBG for pleasant company and collaborations: *Shambunath Bose, Christian Code, Ove Eriksson, Yegor Domanov, Morten Hagen, Arimatti Jutila, Zhu Keng, Antti Metso, Juha-Pekka Mattila, Oula Peñate Medina, Tuula Peñate Medina* (née *Nurminen*)*, Irina Moilanen, Antti Pakkanen, Jussi Pirneskoski, Karen Sabatini, Rohit Sood, Tim Söderlund, Esa Tuominen, Ilkka Tuunainen, and Zhao Hongxia*. Skillful technical assistance by *Kaija Niva* and *Kristiina Söderholm* has been crucial for this work and is highly appreciated. Our secretary *Kaija Tiilikka* has helped me through many bureaucratic obstacles along the way.

I am grateful for professor *Olli Ikkala* and Doc. Dr. *Martin Hof* for reviewing the thesis and providing relevant criticism and comments.

Members of my Thesis Committee professor *Elina Ikonen* and docent *Matti Jauhianen* are acknowledged for guidance during the thesis project.

I have had opportunity to discuss about my project with many prominent researchers in the fields of biophysics and surface science. Professors *Ole Mouritsen*, *Fred Menger*, *Adrian Sutton*, and *Kimmo Kaski* are thanked for especially rewarding discussions.

I wish to express gratitude to my parents *Sirpa* and *Lasse* who have always encouraged me to pursue intellectual goals. My brothers *Jaakko* and *Tapio* are warmly thanked for lifelong friendship and countless hilarious moments. My beloved wife *Eeva* has patiently supported me through ups and downs of the thesis project. Without her love and understanding attitude this work would have been much harder.

Helsinki Biomedical Graduate School provided important economical support in the forms of monthly salaries and travel grants. Thanks are due to former and present head of HBGS, professors *Olli Jänne* and *Tomi Mäkelä*. This study was in part supported by personal grants from the Finnish Medical Foundation, the Research and Science Foundation of Farmos, the Finnish Medical Society Duodecim, and the Emil Aaltonen Foundation. HBBG was supported by TEKES, the Finnish State Medical Research Council, the Finnish Academy, and the Sigrid Jusélius Foundation during my thesis work.

Helsinki, December 2005

Samppa Ryhänen

REFERENCES

Akao, T., Fukumoto, T., Ihara, H., and Ito, A. 1996. Conformational change in DNA induced by cationic bilayer membranes. *FEBS Lett.* 391:215-218.

Alakoskela, J.I. and Kinnunen, P.K.J. 2004. Phospholipid main phase transition assessed by fluorescence spectroscopy. In *Reviews in Fluorescence*, Geddes, C.D. and Lakowicz, J.R., Eds. (Kluwer Academic/Plenum Publishers, New York, USA), pp. 257-297.

Alberts, B., A. Johnson, J. Lewis, M. Raff, K. Roberts, and P. Walter. 2002. Molecular Biology of the Cell. Garland Science, New York, USA.

Allen, T.M. and Cullis, P.R. 2004. Drug delivery systems: entering the mainstream. *Science.* 303:1818-1822.

Allen, T.M. 1998. Liposomal drug formulations. Rationale for development and what we can expect for the future. *Drugs.* 56:747-756.

Allen, T.M. 1997. Liposomes. Opportunities in drug delivery. *Drugs.* 54 Suppl 4:8-14.

Angelova, M. and Dimitrov, D. 1986. Liposome electroformation. *Faraday Discuss.Chem.Soc.* 81:303-311.

Arima, H., Aramaki, Y., and Tsuchiya, S. 1997. Contribution of trypsin-sensitive proteins to binding of cationic liposomes to the mouse macrophage-like cell line RAW264.7. *J.Pharm.Sci.* 86:786-790.

Bagatolli, L.A. 2003. Direct observation of lipid domains in free standing bilayers: from simple to complex lipid mixtures. *Chem.Phys.Lipids.* 122:137-145.

Bally, M.B., Harvie, P., Wong, F.M., Kong, S., Wasan, E.K., and Reimer, D.L. 1999. Biological barriers to cellular delivery of lipid-based DNA carriers. *Adv.Drug Deliv.Rev.* 38:291-315.

Bandyopadhyay, S., Tarek, M., and Klein, M.L. 1999. Molecular dynamics study of a lipid-DNA complex. *J.Phys.Chem. B.* 103:10075-10080.

Bangham, A.D., Standish, M.M., and Watkins, J.C. 1965. Diffusion of univalent ions across the lamellae of swollen phospholipids. *J.Mol.Biol.* 13:238-252.

Belting, M., Sandgren, S., and Wittrup, A. 2005. Nuclear delivery of macromolecules: barriers and carriers. *Adv.Drug Deliv.Rev.* 57:505-527.

Bhattacharya, S. and Mandal, S.S. 1998. Evidence of interlipidic ion-pairing in anion-induced DNA release from cationic amphiphile-DNA complexes. Mechanistic implications in transfection. *Biochemistry.* 37:7764-7777.

Bloomfield, V.A. 1996. DNA condensation. *Curr.Opin.Struct.Biol.* 6:334-341.

Bloomfield, V.A. 1998. DNA condensation by multivalent cations. *Biopolymers.* 44:269-282.

Bloomfield, V.A. 1991. Condensation of DNA by multivalent cations: considerations on mechanism. *Biopolymers.* 31:1471-1481.

Braun, C.S., Jas, G.S., Choosakoonkriang, S., Koe, G.S., Smith, J.G., and Middaugh, C.R. 2003. The structure of DNA within cationic lipid/DNA complexes. *Biophys.J.* 84:1114-1123.

Brockman, H. 1999. Lipid monolayers: why use half a membrane to characterize protein-membrane interactions? *Curr.Opin.Struct.Biol.* 9:438-443.

Budker, V., Gurevich, V., Hagstrom, J.E., Bortzov, F., and Wolff, J.A. 1996. pH-sensitive, cationic liposomes: a new synthetic virus-like vector. *Nat.Biotechnol.* 14:760-764.

Cain, B.F., Baguley, B.C., and Denny, W.A. 1978. Potenial antitumor agents. 28. Deoxyribonucleic acid polyintercalating agents. *J.Med.Chem.* 21:658-668.

Cavazzana-Calvo, M., Hacein-Bey, S., de Saint Basile, G., Gross, F., Yvon, E., Nusbaum, P., Selz, F., Hue, C., Certain, S., Casanova, J.L., Bousso, P., Deist, F.L., and Fischer, A. 2000. Gene therapy of human severe combined immunodeficiency (SCID)-X1 disease. *Science.* 288:669-672.

Cevc, G. 1990. Membrane electrostatics. *Biochim.Biophys.Acta.* 1031:311-382.

Cevc, G., Watts, A., and Marsh, D. 1981. Titration of the phase transition of phosphatidylserine bilayer membranes. Effects of pH, surface electrostatics, ion binding, and head-group hydration. *Biochemistry.* 20:4955-4965.

Chen, T., Wong, K.F., Fenske, D.B., Palmer, L.R., and Cullis, P.R. 2000. Fluorescent-labeled poly(ethylene glycol) lipid conjugates with distal cationic headgroups. *Bioconjug.Chem.* 11:433-437.

Chesnoy, S. and Huang, L. 2000. Structure and function of lipid-DNA complexes for gene delivery. *Annu.Rev.Biophys.Biomol.Struct.* 29:27-47.

Cravatt, B.F., Prospero-Garcia, O., Siuzdak, G., Gilula, N.B., Henriksen, S.J., Boger, D.L., and Lerner, R.A. 1995. Chemical characterization of a family of brain lipids that induce sleep. *Science.* 268:1506-1509.

Dass, C.R. 2004. Lipoplex-mediated delivery of nucleic acids: factors affecting in vivo transfection. *J.Mol.Med.* 82:579-591.

De Smedt, S.C., Demeester, J., and Hennink, W.E. 2000. Cationic polymer based gene delivery systems. *Pharm.Res.* 17:113-126.

de Vries, A.H., Yefimov, S., Mark, A.E., and Marrink, S.J. 2005. Molecular structure of the lecithin ripple phase. *Proc.Natl.Acad.Sci.U.S.A.* 102:5392-5396.

Elouahabi, A., and Ruysschaert, J.M. 2005. Formation and intracellular trafficking of lipoplexes and polyplexes. *Mol.Ther.* 11:336-347.

El Ouahabi, A., Thiry, M., Schiffmann, S., Fuks, R., Nguyen-Tran, H., Ruysschaert, J.M., and Vandenbranden, M. 1999. Intracellular visualization of BrdU-labeled plasmid DNA/cationic liposome complexes. *J.Histochem.Cytochem.* 47:1159-1166.

Evans, E., Bowman, H., Leung, A., Needham, D., and Tirrell, D. 1996. Biomembrane templates for nanoscale conduits and networks. *Science.* 273:933-935.

Evans, E., and Kwok, R. 1982. Mechanical calorimetry of large dimyristoylphosphatidylcholine vesicles in the phase transition region. *Biochemistry.* 21:4874-4879.

Farhood, H., Serbina, N., and Huang, L. 1995. The role of dioleoyl phosphatidylethanolamine in cationic liposome mediated gene transfer. *Biochim.Biophys.Acta.* 1235:289-295.

Felgner, P.L., Barenholz, Y., Behr, J.P., Cheng, S.H., Cullis, P., Huang, L., Jessee, J.A., Seymour, L., Szoka, F., Thierry, A.R., Wagner, E., and Wu, G. 1997. Nomenclature for synthetic gene delivery systems. *Hum.Gene Ther.* 8:511-512.

Felgner, P.L., Gadek, T.R., Holm, M., Roman, R., Chan, H.W., Wenz, M., Northrop, J.P., Ringold, G.M., and Danielsen, M. 1987. Lipofection: a highly efficient, lipid-mediated DNA-transfection procedure. *Proc.Natl.Acad.Sci.U.S.A.* 84:7413-7417.

Fielden, M.L., Perrin, C., Kremer, A., Bergsma, M., Stuart, M.C., Camilleri, P., and Engberts, J.B.F.N. 2001. Sugar-based tertiary amino gemini surfactants with a vesicle-to-micelle transition in the endosomal pH range mediate efficient transfection in vitro. *Eur. J. Biochem.* 268:1269-1279.

Friend, D.S., Papahadjopoulos, D., and Debs, R.J. 1996. Endocytosis and intracellular processing accompanying transfection mediated by cationic liposomes. *Biochim.Biophys.Acta.* 1278:41-50.

Gant, T.M. and Wilson, K.L. 1997. Nuclear assembly. *Annu.Rev.Cell Dev.Biol.* 13:669-695.

Geall, A.J., Eaton, M.A., Baker, T., Catterall, C., and Blagbrough, I.S. 1999. The regiochemical distribution of positive charges along cholesterol polyamine carbamates plays significant roles in modulating DNA binding affinity and lipofection. *FEBS Lett.* 459:337-342.

Gelbart, W.M., Bruinsma, R.F., Pincus, P.A., and Parsegian, V.A. 2000. DNA-inspired electrostatics. *Phys. Today.* 53:38-44.

Gershon, H., Ghirlando, R., Guttman, S.B., and Minsky, A. 1993. Mode of formation and structural features of DNA-cationic liposome complexes used for transfection. *Biochemistry.* 32:7143-7151.

Glover, D.J., Lipps, H.J., and Jans, D.A. 2005. Towards safe, non-viral therapeutic gene expression in humans. *Nat.Rev.Genet.* 6:299-310.

Gluzman, Y. 1981. SV40-transformed simian cells support the replication of early SV40 mutants. *Cell.* 23:175-182.

Griparic, L. and van der Bliek, A.M. 2001. The many shapes of mitochondrial membranes. *Traffic.* 2:235-244.

Gurtovenko, A.A., Patra, M., Karttunen, M., and Vattulainen, I. 2004. Cationic DMPC/DMTAP lipid bilayers: molecular dynamics study. *Biophys.J.* 86:3461-3472.

Haas, S., Hoffmann, H., Thunig, C., and Hoinkis, E. 1999. Phase and aggregation behaviour of double-chain cationic surfactants from the class of N-alkyl-N-alkyl'-N,N-dimethylammonium bromide surfactants. *Colloid Polym.Sci.* 277:856-867.

Hacein-Bey-Abina, S., Le Deist, F., Carlier, F., Bouneaud, C., Hue, C., De Villartay, J.P., Thrasher, A.J., Wulffraat, N., Sorensen, R., Dupuis-Girod, S., Fischer, A., Davies, E.G., Kuis, W., Leiva, L., and Cavazzana-Calvo, M. 2002. Sustained correction of X-linked severe combined immunodeficiency by ex vivo gene therapy. *N.Engl.J.Med.* 346:1185-1193.

Hacein-Bey-Abina, S., von Kalle, C., Schmidt, M., Le Deist, F., Wulffraat, N., McIntyre, E., Radford, I., Villeval, J.L., Fraser, C.C., Cavazzana-Calvo, M., and Fischer, A. 2003a. A serious adverse event after successful gene therapy for X-linked severe combined immunodeficiency. *N.Engl.J.Med.* 348:255-256.

Hacein-Bey-Abina, S., von Kalle, C., Schmidt, M., McCormack, M.P., Wulffraat, N., Leboulch, P., Lim, A., Osborne, C.S., Pawliuk, R., Morillon, E., Sorensen, R., Forster, A., Fraser, P., Cohen, J.I., de Saint Basile, G., Alexander, I., Wintergerst, U., Frebourg, T., Aurias, A., Stoppa-Lyonnet, D., Romana, S., Radford-Weiss, I., Gross, F., Valensi, F., Delabesse, E., Macintyre, E., Sigaux, F., Soulier, J., Leiva, L.E., Wissler, M., Prinz, C., Rabbitts, T.H., Le Deist, F., Fischer, A., and Cavazzana-Calvo, M. 2003b. LMO2-associated clonal T cell proliferation in two patients after gene therapy for SCID-X1. *Science.* 302:415-419.

Hafez, I.M., Maurer, N., and Cullis, P.R. 2001. On the mechanism whereby cationic lipids promote intracellular delivery of polynucleic acids. *Gene Ther.* 8:1188-1196.

Heimburg, T. 1998. Mechanical aspects of membrane thermodynamics. Estimation of the mechanical properties of lipid membranes close to the chain melting transition from calorimetry. *Biochim.Biophys.Acta.* 1415:147-162.

Hirsch-Lerner, D. and Barenholz, Y. 1999. Hydration of lipoplexes commonly used in gene delivery: follow-up by laurdan fluorescence changes and quantification by differential scanning calorimetry. *Biochim.Biophys.Acta.* 1461:47-57.

Holopainen, J.M., Angelova, M., and Kinnunen, P.K.J. 2003. Giant liposomes in studies on membrane domain formation. *Meth.Enzymol.* 367:15-23.

Hui, S.W., Langner, M., Zhao, Y.L., Ross, P., Hurley, E., and Chan, K. 1996. The role of helper lipids in cationic liposome-mediated gene transfer. *Biophys.J.* 71:590-599.

Hutterer, R., Schneider, F.W., and Hof, M. 1997. Anisotropy and lifetime profiles for *n*-anthroyloxy fatty acids: a fluorescence method for the detection of bilayer interdigitation. *Chem.Phys.Lipids.* 86:51-64.

Israelachvili, J. 1991. Intermolecular & Surface Forces. 2nd ed., Academic Press, London.

Israelachvili, J.N., Marcelja, S., and Horn, R.G. 1980. Physical principles of membrane organization. *Q.Rev.Biophys.* 13:121-200.

Kaganer, V.M., Möhwald, H., and Dutta, P. 1999. Structure and phase transitions in Langmuir monolayers. *Rev. Mod. Phys.* 71:779-819.

Kikuchi, I.S. and Carmona-Ribeiro, A.M. 2000. Interactions between DNA and synthetic cationic liposomes. *J.Phys.Chem. B.* 104:2829-2835.

Kinnunen, P.K.J. 1991. On the principles of functional ordering in biological membranes. *Chem.Phys.Lipids.* 57:375-399.

Kinnunen, P.K.J. 1996. On the mechanisms of the lamellar -> hexagonal HII phase transition and the biological significance of the HII propensity. In *Handbook of Nonmedical Applications of Liposomes*, Lasic, D.D. and Barenholz, Y., Eds. (CRC Press, Boca Raton, USA), pp. 153-171.

Kinnunen, P.K.J. and Holopainen, J.M. 2000. Mechanisms of initiation of membrane fusion: role of lipids. *Biosci.Rep.* 20:465-482.

Kinnunen, P.K.J., Kõiv, A., Lehtonen, J.Y., Rytömaa, M., and Mustonen, P. 1994. Lipid dynamics and peripheral interactions of proteins with membrane surfaces. *Chem.Phys.Lipids.* 73:181-207.

Kinnunen, P.K.J. and Laggner, P. 1991. Special issue on phospholipid phase transitions. *Chem. Phys. Lipids.* 57:109-408.

Kinnunen, P.K.J., Rytömaa, M., Kõiv, A., Lehtonen, J., Mustonen, P., and Aro, A. 1993. Sphingosine-mediated membrane association of DNA and its reversal by phosphatidic acid. *Chem.Phys.Lipids.* 66:75-85.

Kirby, A.J., Camilleri, P., Engberts, J.B.F.N., Feiters, M.C., Nolte, R.J.M., Soderman, O., Bergsma, M., Bell, P.C., Fielden, M.L., Garcia Rodriguez, C.L., Guedat, P., Kremer, A., McGregor, C., Perrin, C., Ronsin, G., and van Eijk, M.C.P. 2003. Gemini surfactants: new synthetic vectors for gene transfection. *Angew. Chem.-Int. Edit.* 42:1448-1457.

Kleinschmidt, J.H., Powell, G.L., and Marsh, D. 1998. Cytochrome c-induced increase of motionally restricted lipid in reconstituted cytochrome c oxidase membranes, revealed by spin-label ESR spectroscopy. *Biochemistry.* 37:11579-11585.

Kõiv, A. and Kinnunen, P.K. 1994. Binding of DNA to liposomes containing different derivatives of sphingosine. *Chem.Phys.Lipids.* 72:77-86.

Kõiv, A., Mustonen, P., and Kinnunen, P.K.J. 1994. Differential scanning calorimetry study on the binding of nucleic acids to dimyristoylphosphatidylcholine-sphingosine liposomes. *Chem.Phys.Lipids.* 70:1-10.

Kõiv, A., Mustonen, P., and Kinnunen, P.K.J. 1993. Influence of sphingosine on the thermal phase behaviour of neutral and acidic phospholipid liposomes. *Chem.Phys.Lipids.* 66:123-134.

Kõiv, A., Palvimo, J., and Kinnunen, P.K.J. 1995. Evidence for ternary complex formation by histone H1, DNA, and liposomes. *Biochemistry.* 34:8018-8027.

Koltover, I., Salditt, T., Rädler, J.O., and Safinya, C.R. 1998. An inverted hexagonal phase of cationic liposome-DNA complexes related to DNA release and delivery. *Science.* 281:78-81.

Koynova, R. and MacDonald, R.C. 2004. Columnar DNA Superlattices in Lamellar o-Ethylphosphatidylcholine Lipoplexes: Mechanism of the Gel-Liquid Crystalline Lipid Phase Transition. *Nano Letters.* 4:1475-1479.

Koynova, R. and MacDonald, R.C. 2003. Mixtures of cationic lipid O-ethylphosphatidylcholine with membrane lipids and DNA: phase diagrams. *Biophys.J.* 85:2449-2465.

Kunz, W., Henle, J., and Ninham, B.W. 2004a. 'Zur Lehre von der Wirkung der Salze' (About the science of the effect of salts): Franz Hofmeister's historical papers. *Curr.Opin. Colloid Interface Sci.* 9:19-37.

Kunz, W., Lo Nostro, P., and Ninham, B.W. 2004b. The present state of affairs with Hofmeister effects. *Curr.Opin. Colloid Interface Sci.* 9:1-18.

Lakowicz, J.R., Prendergast, F.G., and Hogen, D. 1979a. Differential polarized phase fluorometric investigations of diphenylhexatriene in lipid bilayers. Quantitation of hindered depolarizing rotations. *Biochemistry.* 18:508-519.

Lakowicz, J.R., Prendergast, F.G., and Hogen, D. 1979b. Fluorescence anisotropy measurements under oxygen quenching conditions as a method to quantify the depolarizing rotations of

fluorophores. Application to diphenylhexatriene in isotropic solvents and in lipid bilayers. *Biochemistry.* 18:520-527.

Lakowicz, J.R. 1999. Principles of Fluorescence Spectroscopy. 2nd ed., Kluwer Academic / Plenum Publishers, USA.

Landh, T. 1995. From entangled membranes to eclectic morphologies: cubic membranes as subcellular space organizers. *FEBS Lett.* 369:13-17.

Langmuir, I. 1917. Constitution and fundamental properties of solids and liquids. II. Liquids. *J.Am.Chem.Soc.* 39:1848-1906.

Langner, M. and Kubica, K. 1999. The electrostatics of lipid surfaces. *Chem.Phys.Lipids.* 101:3-35.

Lechardeur, D., Sohn, K.J., Haardt, M., Joshi, P.B., Monck, M., Graham, R.W., Beatty, B., Squire, J., O'Brodovich, H., and Lukacs, G.L. 1999. Metabolic instability of plasmid DNA in the cytosol: a potential barrier to gene transfer. *Gene Ther.* 6:482-497.

Lehtonen, J.Y., Holopainen, J.M., and Kinnunen, P.K.J. 1996. Evidence for the formation of microdomains in liquid crystalline large unilamellar vesicles caused by hydrophobic mismatch of the constituent phospholipids. *Biophys.J.* 70:1753-1760.

Lehtonen, J.Y. and Kinnunen, P.K.J. 1995. Poly(ethylene glycol)-induced and temperature-dependent phase separation in fluid binary phospholipid membranes. *Biophys.J.* 68:525-535.

Leidy, C., Kaasgaard, T., Crowe, J.H., Mouritsen, O.G., and Jorgensen, K. 2002. Ripples and the formation of anisotropic lipid domains: imaging two-component supported double bilayers by atomic force microscopy. *Biophys.J.* 83:2625-2633.

Lewis, R.N. and McElhaney, R.N. 1996. Fourier Transform Infrared Spectroscopy in the Study of Hydrated Lipids and Lipid Bilayer Membranes. In *Infrared Spectroscopy of Biomolecules*, Mantsch, H.H. and Chapman, D., Eds. (Wiley-Liss, Hoboken, USA), pp. 159-202.

Lewis, R.N. and McElhaney, R.N. 2000. Surface charge markedly attenuates the nonlamellar phase-forming propensities of lipid bilayer membranes: calorimetric and (31)P-nuclear magnetic resonance studies of mixtures of cationic, anionic, and zwitterionic lipids. *Biophys.J.* 79:1455-1464.

Lewis, R.N., Winter, I., Kriechbaum, M., Lohner, K., and McElhaney, R.N. 2001. Studies of the structure and organization of cationic lipid bilayer membranes: calorimetric, spectroscopic, and x-ray diffraction studies of linear saturated P-O-ethyl phosphatidylcholines. *Biophys.J.* 80:1329-1342.

Lin, A.J., Slack, N.L., Ahmad, A., George, C.X., Samuel, C.E., and Safinya, C.R. 2003. Three-dimensional imaging of lipid gene-carriers: membrane charge density controls universal transfection behavior in lamellar cationic liposome-DNA complexes. *Biophys.J.* 84:3307-3316.

Lin, K.C., Weis, R.M., and McConnell, H.M. 1982. Induction of helical liposomes by Ca^{2+}-mediated intermembrane binding. *Nature.* 296:164-165.

Luchetti, L. and Mancini, G. 2000. NMR Investigation on the various aggregates formed by a gemini chiral surfactant. *Langmuir.* 16:161-165.

Luisi, P.L., Walde, P., and Oberholzer, T. 1999. Lipid vesicles as possible intermediates in the origin of life. *Curr.Opin. Colloid Interface Sci.* 4:33-39.

MacDonald, R.C., MacDonald, R.I., Menco, B.P., Takeshita, K., Subbarao, N.K., and Hu, L.R. 1991. Small-volume extrusion apparatus for preparation of large, unilamellar vesicles. *Biochim.Biophys.Acta.* 1061:297-303.

Matulis, D., Rouzina, I., and Bloomfield, V.A. 2002. Thermodynamics of cationic lipid binding to DNA and DNA condensation: roles of electrostatics and hydrophobicity. *J.Am.Chem.Soc.* 124:7331-7342.

McElhaney, R.N. 1982. The use of differential scanning calorimetry and differential thermal analysis in studies of model and biological membranes. *Chem.Phys.Lipids.* 30:229-259.

Menger, F.M. and Angelova, M.I. 1998. Giant vesicles: imitating the cytological processes of cell membranes. *Acc.Chem.Res.* 31:789-797.

Menger, F.M. and Gabrielson, K.D. 1995. Cytomimetic organic chemistry: early developments. *Angew. Chem.-Int. Edit.* 34:2091-2106.

Menger, F.M. and Keiper, J.S. 1998. Chemistry and physics of giant vesicles as biomembrane models. *Curr.Opin.Chem.Biol.* 2:726-732.

Menger, F.M. and Keiper, J.S. 2000. Gemini surfactants. *Angew. Chem.-Int. Edit.* 39:1907-1920.

Menger, F.M. and Littau, C.A. 1993. Gemini surfactants: a new class of self-assembling molecules. *J.Am.Chem.Soc.* 115:10083-10090.

Menger, F.M. and Mbadugha, B.N.A. 2001. Gemini surfactants with a disaccharide spacer. *J.Am.Chem.Soc.* 123:875-885.

Menger, F.M. and Peresypkin, A.V. 2001. A combinatorially-derived structural phase diagram for 42 zwitterionic geminis. *J.Am.Chem.Soc.* 123:5614-5615.

Menger, F.M., Peresypkin, A.V., Caran, K.L., and Apkarian, R.P. 2000. A sponge morphology in an elementary coacervate. *Langmuir.* 16:9113-9116.

Meyer, O., Kirpotin, D., Hong, K., Sternberg, B., Park, J.W., Woodle, M.C., and Papahadjopoulos, D. 1998. Cationic liposomes coated with polyethylene glycol as carriers for oligonucleotides. *J.Biol.Chem.* 273:15621-15627.

Mislick, K.A. and Baldeschwieler, J.D. 1996. Evidence for the role of proteoglycans in cation-mediated gene transfer. *Proc.Natl.Acad.Sci.U.S.A.* 93:12349-12354.

Mok, K.W. and Cullis, P.R. 1997. Structural and fusogenic properties of cationic liposomes in the presence of plasmid DNA. *Biophys.J.* 73:2534-2545.

Mortimer, I., Tam, P., MacLachlan, I., Graham, R.W., Saravolac, E.G., and Joshi, P.B. 1999. Cationic lipid-mediated transfection of cells in culture requires mitotic activity. *Gene Ther.* 6:403-411.

Mounkes, L.C., Zhong, W., Cipres-Palacin, G., Heath, T.D., and Debs, R.J. 1998. Proteoglycans mediate cationic liposome-DNA complex-based gene delivery in vitro and in vivo. *J.Biol.Chem.* 273:26164-26170.

Mouritsen, O.G. 2005. Life as a Matter of Fat: The Emerging Science of Lipidomics. Springer-Verlag, Berlin and Heidelberg.

Mouritsen, O.G. and Bloom, M. 1984. Mattress model of lipid-protein interactions in membranes. *Biophys.J.* 46:141-153.

Mouritsen, O.G. and Kinnunen, P.K.J. 1996. Role of lipid organization and dynamics for membrane functionality. In *Biological Membranes*, Merz, K.M. and Roux, B., Eds. (Birkhäuser, Boston, USA), pp. 463-502.

Mouritsen, O.G. and Zuckermann, M.J. 2004. What's so special about cholesterol? *Lipids.* 39:1101-1113.

Nagle, J.F. and Tristram-Nagle, S. 2000. Structure of lipid bilayers. *Biochim.Biophys.Acta.* 1469:159-195.

Nambi, P., Rowe, E.S., and McIntosh, T.J. 1988. Studies of the ethanol-induced interdigitated gel phase in phosphatidylcholines using the fluorophore 1,6-diphenyl-1,3,5-hexatriene. *Biochemistry.* 27:9175-9182.

Needham, D. and Evans, E. 1988. Structure and mechanical properties of giant lipid (DMPC) vesicle bilayers from 20 ^{o}C below to 10 ^{o}C above the liquid crystal-crystalline phase transition at 24 ^{o}C. *Biochemistry.* 27:8261-8269.

Niven, R., Pearlman, R., Wedeking, T., Mackeigan, J., Noker, P., Simpson-Herren, L., and Smith, J.G. 1998. Biodistribution of radiolabeled lipid-DNA complexes and DNA in mice. *J.Pharm.Sci.* 87:1292-1299.

O'Leary, T.J. and Levin, I.W. 1984. Raman spectroscopic study of an interdigitated lipid bilayer. Dipalmitoylphosphatidylcholine dispersed in glycerol. *Biochim.Biophys.Acta.* 776:185-189.

Parker, S.E., Ducharme, S., Norman, J., and Wheeler, C.J. 1997. Tissue distribution of the cytofectin component of a plasmid-DNA/cationic lipid complex following intravenous administration in mice. *Hum.Gene Ther.* 8:393-401.

Pascher, I., Lundmark, M., Nyholm, P.G., and Sundell, S. 1992. Crystal structures of membrane lipids. *Biochim.Biophys.Acta.* 1113:339-373.

Paukku, T., Lauraeus, S., Huhtaniemi, I., and Kinnunen, P.K. 1997. Novel cationic liposomes for DNA-transfection with high efficiency and low toxicity. *Chem.Phys.Lipids.* 87:23-29.

Pebay-Peyroula, E., Dufourc, E.J., and Szabo, A.G. 1994. Location of diphenyl-hexatriene and trimethylammonium-diphenyl-hexatriene in dipalmitoylphosphatidylcholine bilayers by neutron diffraction. *Biophys.Chem.* 53:45-56.

Peñate Medina, O., Zhu, Y., and Kairemo, K. 2004. Targeted liposomal drug delivery in cancer. *Curr.Pharm.Des.* 10:2981-2989.

Pohle, W., Selle, C., Gauger, D.R., Zantl, R., Artzner, F., and Rädler, J.O. 2000. FTIR spectroscopic characterization of a cationic lipid-DNA complex and its components. *Physical Chemistry Chemical Physics.* 2:4642-4650.

Pollard, H., Remy, J.S., Loussouarn, G., Demolombe, S., Behr, J.P., and Escande, D. 1998. Polyethylenimine but not cationic lipids promotes transgene delivery to the nucleus in mammalian cells. *J.Biol.Chem.* 273:7507-7511.

Raper, S.E., Chirmule, N., Lee, F.S., Wivel, N.A., Bagg, A., Gao, G.P., Wilson, J.M., and Batshaw, M.L. 2003. Fatal systemic inflammatory response syndrome in a ornithine transcarbamylase deficient patient following adenoviral gene transfer. *Mol.Genet.Metab.* 80:148-158.

Reddy, J.A., Abburi, C., Hofland, H., Howard, S.J., Vlahov, I., Wils, P., and Leamon, C.P. 2002. Folate-targeted, cationic liposome-mediated gene transfer into disseminated peritoneal tumors. *Gene Ther.* 9:1542-1550.

Reimer, D.L., Kong, S., and Bally, M.B. 1997. Analysis of cationic liposome-mediated interactions of plasmid DNA with murine and human melanoma cells in vitro. *J.Biol.Chem.* 272:19480-19487.

Rejman, J., Oberle, V., Zuhorn, I.S., and Hoekstra, D. 2004. Size-dependent internalization of particles via the pathways of clathrin- and caveolae-mediated endocytosis. *Biochem.J.* 377:159-169.

Ross, P.C. and Hui, S.W. 1999. Lipoplex size is a major determinant of in vitro lipofection efficiency. *Gene Ther.* 6:651-659.

Ross, P.C., Hensen, M.L., Supabphol, R., and Hui, S.W. 1998. Multilamellar cationic liposomes are efficient vectors for in vitro gene transfer in serum. *J.Liposome Res.* 8:499-520.

Ryhänen, S.J., Pakkanen, A.L., Säily, M.J., Bello, C., Mancini, G., and Kinnunen, P.K.J. 2002. Impact of the stereochemical structure on the thermal phase behavior of a cationic gemini surfactant. *J.Phys.Chem. B.* 106:11694-11697.

Säily, V.M.J., Alakoskela, J., Ryhänen, S.J., Karttunen, M., and Kinnunen, P.K.J. 2003. Characterization of sphingosine-phosphatidylcholine monolayers: effects of DNA. *Langmuir.* 19:8956-8963.

Scherer, P.G. and Seelig, J. 1989. Electric charge effects on phospholipid headgroups. Phosphatidylcholine in mixtures with cationic and anionic amphiphiles. *Biochemistry.* 28:7720-7728.

Seelig, J., Macdonald, P.M., and Scherer, P.G. 1987. Phospholipid head groups as sensors of electric charge in membranes. *Biochemistry.* 26:7535-7541.

Shi, N., Zhang, Y., Zhu, C., Boado, R.J., and Pardridge, W.M. 2001. Brain-specific expression of an exogenous gene after i.v. administration. *Proc.Natl.Acad.Sci.U.S.A.* 98:12754-12759.

Shimshick, E.J. and McConnell, H.M. 1973. Lateral phase separation in phospholipid membranes. *Biochemistry.* 12:2351-2360.

Silvius, J.R. 1991. Anomalous mixing of zwitterionic and anionic phospholipids with double-chain cationic amphiphiles in lipid bilayers. *Biochim.Biophys.Acta.* 1070:51-59.

Simberg, D., Weisman, S., Talmon, Y., Faerman, A., Shoshani, T., and Barenholz, Y. 2003. The role of organ vascularization and lipoplex-serum initial contact in intravenous murine lipofection. *J.Biol.Chem.* 278:39858-39865.

Simoes, S., Pires, P., Duzgunes, N., and De Lima, M.C.P. 1999. Cationic liposomes as gene transfer vectors: Barriers to successful application in gene therapy. *Curr.Opin.Mol.Ther.* 1:147-157.

Simons, K., and Ikonen, E. 1997. Functional rafts in cell membranes. *Nature.* 387:569-572.

Singer, S.J., and Nicolson, G.L. 1972. The fluid mosaic model of the structure of cell membranes. *Science.* 175:720-731.

Smisterova, J., Wagenaar, A., Stuart, M.C., Polushkin, E., ten Brinke, G., Hulst, R., Engberts, J.B., and Hoekstra, D. 2001. Molecular shape of the cationic lipid controls the structure of cationic

lipid/dioleylphosphatidylethanolamine-DNA complexes and the efficiency of gene delivery. *J.Biol.Chem.* 276:47615-47622.

Sommerdijk, N.A.J.M., Hoeks, T.H.L., Synak, M., Feiters, M.C., Nolte, R.J.M., and Zwanenburg, B. 1997. Stereodependent fusion and fission of vesicles: calcium binding of synthetic gemini phospholipids containing two phosphate groups. *J.Am.Chem.Soc.* 119:4338-4344.

Soutschek, J., Akinc, A., Bramlage, B., Charisse, K., Constien, R., Donoghue, M., Elbashir, S., Geick, A., Hadwiger, P., Harborth, J., John, M., Kesavan, V., Lavine, G., Pandey, R.K., Racie, T., Rajeev, K.G., Rohl, I., Toudjarska, I., Wang, G., Wuschko, S., Bumcrot, D., Koteliansky, V., Limmer, S., Manoharan, M., and Vornlocher, H.P. 2004. Therapeutic silencing of an endogenous gene by systemic administration of modified siRNAs. *Nature.* 432:173-178.

Sternberg, B., Sorgi, F.L., and Huang, L. 1994. New structures in complex formation between DNA and cationic liposomes visualized by freeze-fracture electron microscopy. *FEBS Lett.* 356:361-366.

Straubinger, R.M., Hong, K., Friend, D.S., and Papahadjopoulos, D. 1983. Endocytosis of liposomes and intracellular fate of encapsulated molecules: encounter with a low pH compartment after internalization in coated vesicles. *Cell.* 32:1069-1079.

Suh, J., Wirtz, D., and Hanes, J. 2003. Efficient active transport of gene nanocarriers to the cell nucleus. *Proc.Natl.Acad.Sci.U.S.A.* 100:3878-3882.

Sumida, Y., Masuyama, A., Oki, T., Kida, T., Nakatsuji, Y., Ikeda, I., and Nojima, M. 1996. Pressure-area isotherms for double-chain amphiphiles bearing two hydroxyl groups derived from diepoxides. *Langmuir.* 12:3986-3990.

Sun, W.J., Tristram-Nagle, S., Suter, R.M., and Nagle, J.F. 1996. Structure of the ripple phase in lecithin bilayers. *Proc.Natl.Acad.Sci.U.S.A.* 93:7008-7012.

Szostak, J.W., Bartel, D.P., and Luisi, P.L. 2001. Synthesizing life. *Nature.* 409:387-390.

Tandia, B.M., Lonez, C., Vandenbranden, M., Ruysschaert, J.M., and Elouahabi, A. 2005. Lipid mixing between lipoplexes and plasma lipoproteins is a major barrier for intravenous transfection mediated by cationic lipids. *J.Biol.Chem.* 280:12255-12261.

Tandia, B.M., Vandenbranden, M., Wattiez, R., Lakhdar, Z., Ruysschaert, J.M., and Elouahabi, A. 2003. Identification of human proteins that bind to cationic lipid/DNA complex and analysis of their effects on transfection efficiency: implications for intravenous gene transfer. *Mol.Ther.* 8:264-273.

Tam, P., Monck, M., Lee, D., Ludkovski, O., Leng, E.C., Clow, K., Stark, H., Scherrer, P., Graham, R.W., and Cullis, P.R. 2000. Stabilized plasmid-lipid particles for systemic gene therapy. *Gene Ther.* 7:1867-1874.

Tate, M.W., Eikenberry, E.F., Turner, D.C., Shyamsunder, E., and Gruner, S.M. 1991. Nonbilayer phases of membrane lipids. *Chem.Phys.Lipids.* 57:147-164.

Thomas, C.E., Ehrhardt, A., and Kay, M.A. 2003. Progress and problems with the use of viral vectors for gene therapy. *Nat.Rev.Genet.* 4:346-358.

Tseng, W.C., Haselton, F.R., and Giorgio, T.D. 1999. Mitosis enhances transgene expression of plasmid delivered by cationic liposomes. *Biochim.Biophys.Acta.* 1445:53-64.

Wagner, K., Harries, D., May, S., Kahl, V., Rädler, J.O., and Ben-Shaul, A. 2000. Direct evidence for counterion release upon cationic lipid-DNA condensation. *Langmuir.* 16:303-306.

Weis, R.M. 1991. Fluorescence microscopy of phospholipid monolayer phase transitions. *Chem.Phys.Lipids.* 57:227-239.

Wiedmer, S.K., Hautala, J., Holopainen, J.M., Kinnunen, P.K., and Riekkola, M.L. 2001. Study on liposomes by capillary electrophoresis. *Electrophoresis.* 22:1305-1313.

Winter, I., Pabst, G., Rappolt, M., and Lohner, K. 2001. Refined structure of 1,2-diacyl-P-O-ethylphosphatidylcholine bilayer membranes. *Chem.Phys.Lipids.* 112:137-150.

Wrobel, I., and Collins, D. 1995. Fusion of cationic liposomes with mammalian cells occurs after endocytosis. *Biochim.Biophys.Acta.* 1235:296-304.

Xu, Y., and Szoka, F.C.,Jr. 1996. Mechanism of DNA release from cationic liposome/DNA complexes used in cell transfection. *Biochemistry.* 35:5616-5623.

Zabner, J., Fasbender, A.J., Moninger, T., Poellinger, K.A., and Welsh, M.J. 1995. Cellular and molecular barriers to gene transfer by a cationic lipid. *J.Biol.Chem.* 270:18997-19007.

Zantl, R., Baicu, L., Artzner, F., Sprenger, I., Rapp, G., and Rädler, J.O. 1999. Thermotropic phase behavior of cationic lipid-DNA complexes compared to binary lipid mixtures. *J.Phys.Chem. B.* 103:10300-10310.

Zelphati, O. and Szoka, F.C.,Jr. 1996. Mechanism of oligonucleotide release from cationic liposomes. *Proc.Natl.Acad.Sci.U.S.A.* 93:11493-11498.

Zelphati, O., Uyechi, L.S., Barron, L.G., and Szoka, F.C.,Jr. 1998. Effect of serum components on the physico-chemical properties of cationic lipid/oligonucleotide complexes and on their interactions with cells. *Biochim.Biophys.Acta.* 1390:119-133.

Zhang, Y.P., Sekirov, L., Saravolac, E.G., Wheeler, J.J., Tardi, P., Clow, K., Leng, E., Sun, R., Cullis, P.R., and Scherrer, P. 1999. Stabilized plasmid-lipid particles for regional gene therapy: formulation and transfection properties. *Gene Ther.* 6:1438-1447.

Zhao, H., Tuominen, E.K., and Kinnunen, P.K. 2004. Formation of amyloid fibers triggered by phosphatidylserine-containing membranes. *Biochemistry.* 43:10302-10307.

Zuhorn, I.S., and Hoekstra, D. 2002. On the mechanism of cationic amphiphile-mediated transfection. To fuse or not to fuse: is that the question? *J.Membr.Biol.* 189:167-179.

Zuhorn, I.S., Kalicharan, R., and Hoekstra, D. 2002a. Lipoplex-mediated transfection of mammalian cells occurs through the cholesterol-dependent clathrin-mediated pathway of endocytosis. *J.Biol.Chem.* 277:18021-18028.

Zuhorn, I.S., Visser, W.H., Bakowsky, U., Engberts, J.B., and Hoekstra, D. 2002b. Interference of serum with lipoplex-cell interaction: modulation of intracellular processing. *Biochim.Biophys.Acta.* 1560:25-36.

Zuidam, N.J., Hirsch-Lerner, D., Margulies, S., and Barenholz, Y. 1999. Lamellarity of cationic liposomes and mode of preparation of lipoplexes affect transfection efficiency. *Biochim.Biophys.Acta.* 1419:207-220.

Zuidam, N.J. and Barenholz, Y. 1997. Electrostatic parameters of cationic liposomes commonly used for gene delivery as determined by 4-heptadecyl-7-hydroxycoumarin. *Biochim.Biophys.Acta.* 1329:211-222.